Initiation of Viscous Detonation

Christopher M. Romick,
University of Notre Dame, Notre Dame, IN

Tariq D. Aslam,
Los Alamos National Laboratory, Los Alamos, NM

and

Joseph M. Powers

University of Notre Dame, Notre Dame, IN

2013 SIAM International Conference on Numerical Combustion

San Antonio, Texas

April 9, 2013

Motivation:

- A standard result from non-linear dynamics is that small phenomena can cascade to affect large phenomena
- Might the small scale phenomenon of physical diffusion play an important role in determining inherent scales in the ignition process of detonation from an initially slow moving flame
- After initiation, detonations nearly universally exhibit instability, giving rise to complex dynamics; in order, to capture these dynamics all inherent length scales must be properly resolved
- In one-step kinetics, the number of points in steady $L_{1/2}$ is used as standard reference for the resolution of a simulation; however, the dynamics of the detonation cause the predicted $L_{1/2}$ to vary in time
- Additional complexity is added when studying detailed kinetics, as it gives rise to multiple intrinsic length scales

Unsteady, Compressible, Reactive Navier-Stokes (NS) Equations

$$\frac{\partial \rho}{\partial t} + \nabla \cdot (\rho \mathbf{u}) = 0,$$

$$\frac{\partial}{\partial t}(\rho \mathbf{u}) + \nabla \cdot (\rho \mathbf{u}\mathbf{u} + p\mathbf{I} - \boldsymbol{\tau}) = \mathbf{0},$$

$$\frac{\partial}{\partial t}\left(\rho\left(e + \frac{\mathbf{u}\cdot\mathbf{u}}{2}\right)\right) + \nabla \cdot \left(\rho \mathbf{u}\left(e + \frac{\mathbf{u}\cdot\mathbf{u}}{2}\right) + (p\mathbf{I} - \boldsymbol{\tau})\cdot\mathbf{u} + \mathbf{q}\right) = 0,$$

$$\frac{\partial}{\partial t}(\rho Y_i) + \nabla \cdot (\rho \mathbf{u} Y_i + \mathbf{j}_i) = \overline{M_i}\dot{\omega}_i,$$

$$p = \mathcal{R}T \sum_{i=1}^{N} \frac{Y_i}{\overline{M_i}}, \qquad e = e\left(T, Y_i\right), \qquad \dot{\omega}_i = \dot{\omega}_i\left(T, Y_i\right),$$

$$\mathbf{j}_i = \rho \sum_{\substack{k=1 \\ k\neq i}}^{N} \frac{\overline{M_i} D_{ik} Y_k}{\overline{M}} \left(\frac{\nabla y_k}{y_k} + \left(1 - \frac{\overline{M_k}}{\overline{M}}\right)\frac{\nabla p}{p}\right) - \frac{D_i^T \nabla T}{T},$$

$$\boldsymbol{\tau} = \mu\left(\nabla \mathbf{u} + (\nabla \mathbf{u})^T - \frac{2}{3}(\nabla \cdot \mathbf{u})\mathbf{I}\right),$$

$$\mathbf{q} = -k\nabla T + \sum_{i=1}^{N} \mathbf{j}_i h_i - \mathcal{R}T \sum_{i=1}^{N} \frac{D_i^T}{\overline{M_i}} \left(\frac{\nabla \overline{y}_i}{\overline{y}_i} + \left(1 - \frac{\overline{M_i}}{\overline{M}}\right)\frac{\nabla p}{p}\right).$$

Computational Methods

- Inviscid
  - Fifth order shock-fitting algorithm, adapted from Henrick *et al.* (*J. Comp. Phys.*, 2006), assures numerical errors are minimal
  - Shock-capturing using WENO5M
  - Both methods use a fifth order Runge-Kutta scheme for time integration
- Viscous
  - Using WAMR, Vasilyev and Paolucci (*JCP*, 1996,1997), which is an adaptive mesh refinement technique utilizing wavelet functions
  - Using a 5th order WENO scheme for advective terms and a 4th order central difference scheme for diffusive terms
  - Utilized either a fifth order Runge-Kutta scheme or a second order Runge-Kutta-Legrendre scheme employing a Strang operator split for time integration

Model Parameters

Hydrogen-Air Detailed Kinetics

$$p_o = 1\,atm$$
$$T_o = 293\,K$$
$$L_{induct} = 1.9 \times 10^{-2}\,cm$$
$$D_{CJ} \approx 1993\,m/s$$
$$f_{cr} \approx 1.2$$

Powers & Paolucci (*AIAAJ*, 2005)

One-step

Set # 1

$$\gamma = 1.17$$
$$M = 21\,g/mol$$
$$E_a = 46.37,\, q = 43.28$$
$$p_o = 1\,atm$$
$$T_o = 293\,K$$
$$L_{1/2} = 1.927 \times 10^{-2}\,cm$$
$$D_{CJ} = 1993\,m/s$$
$$E_{a_{cr}} = 19.21$$

Gamezo et al. (*Comb. & Flame*, 2008)

Set # 2

$$\gamma = 1.4$$
$$M = 28\,g/mol$$
$$E_a = \text{various}, q = 21$$
$$p_o = 1\,atm$$
$$T_o = 300\,K$$
$$L_{1/2} = 1.665 \times 10^{-2}\,cm$$
$$D_{CJ} = 1991\,m/s$$
$$E_{a_{cr}} = 36.01$$

Kassoy et al. (*CTM*, 2008;*CTM*, 2012)

Set # 3

$$\gamma = 1.2$$
$$M = 24\,g/mol$$
$$E_a = \text{various},\, q = 50$$
$$p_o = 1\,atm$$
$$T_o = 293\,K$$
$$L_{1/2} = 2 \times 10^{-2}\,cm$$
$$D_{CJ} = 2167\,m/s$$
$$E_{a_{cr}} = 25.26$$

Henrick et al. (*JCP*, 2006)

Energy Deposition Function

$$\rho Q = \begin{cases} 0 & 0 \le x \le x_i - 2L_z \\ 2.1 \frac{\rho_o a_o^2}{t_a} \cos\left(\frac{\pi}{4L_z}\left(x_i - x\right)\right) & \\ \quad \left(\tanh\left[\frac{5}{2t_a}\left(2t - t_a\right)\right]\right. & \\ \quad \left. - \tanh\left[\frac{5}{2t_a}\left(2t - 20t_a\right)\right]\right) & x_i - 2L_z \le x \le x_i + 2L_z \\ 0 & x < x_i + 2L_z \end{cases}$$

$$\int_{x_i - 2L_z}^{x_i + 2L_z} \int_0^{11t_a} \rho Q \, dt \, dx \approx 5 \times 10^3 \, J/m^2; \qquad L_z / L_{1/2} \approx 2$$

- When the time scale of heat addition is on the order of the local ambient acoustic time scale, partial inertial confinement transpires, leading to a moderately localized pressure increase in spite of simultaneous expansion
- The pressure increase generates compression waves which coalesce to form a shock and cause hot spot formation
- At the same time, a chemical explosion occurs within the region of energy deposition yielding an initial reaction wave traveling slower than the shock

Kassoy et al. (*CTM*, 2008;*CTM*, 2012)

Inviscid Initiation - Parameter Set #2 - $E_a = 13.8$

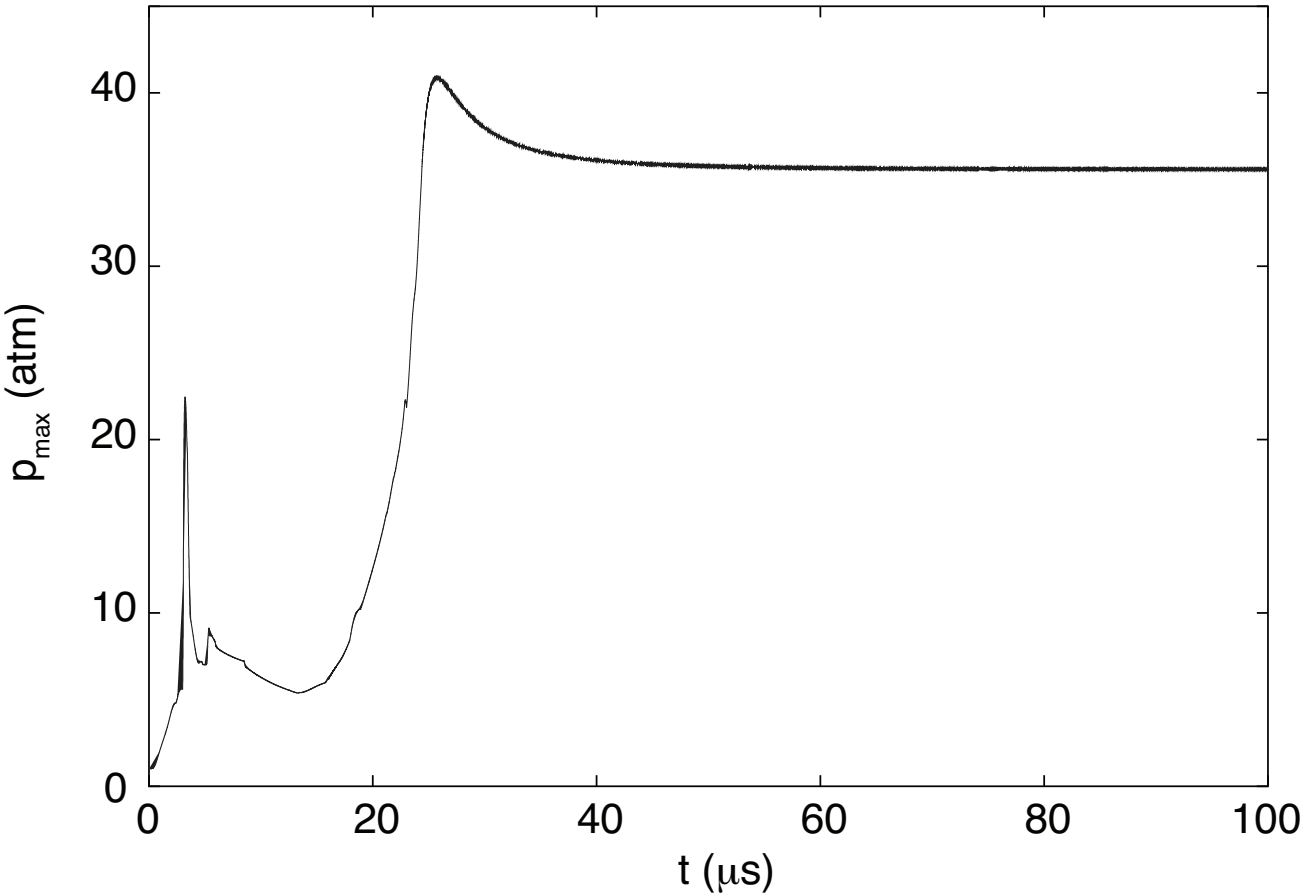

The peak pressure of $40.9\ atm$ occurs at $25.7\ \mu s$.

Inviscid Initiation - $E_a = 14, 15$

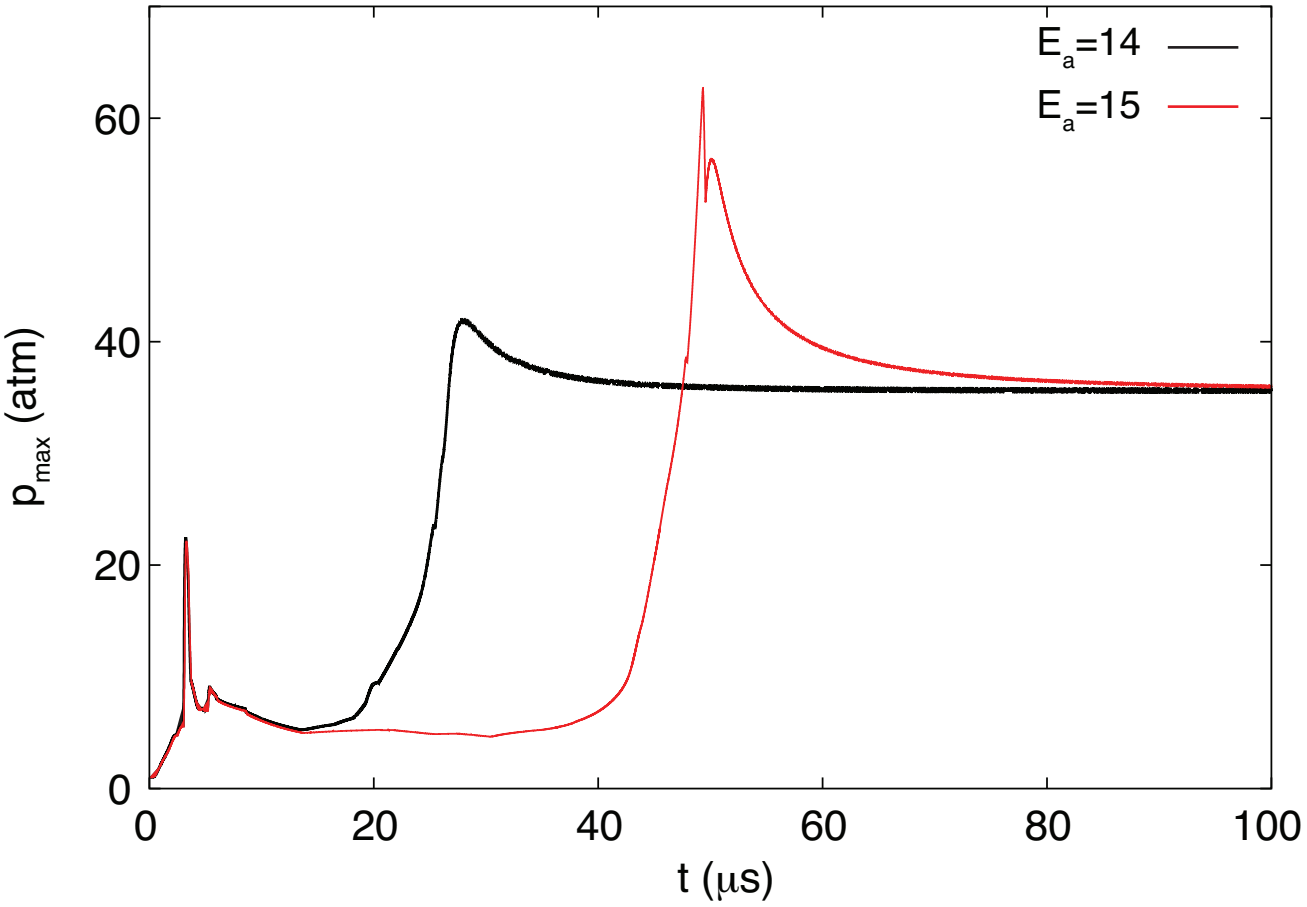

The peak pressure for $E_a = 14$ is $41.6\ atm$ at $28.0\ \mu s$, and for $E_a = 15$ is $62.7\ atm$ at $49.3\ \mu s$.

Inviscid Initiation

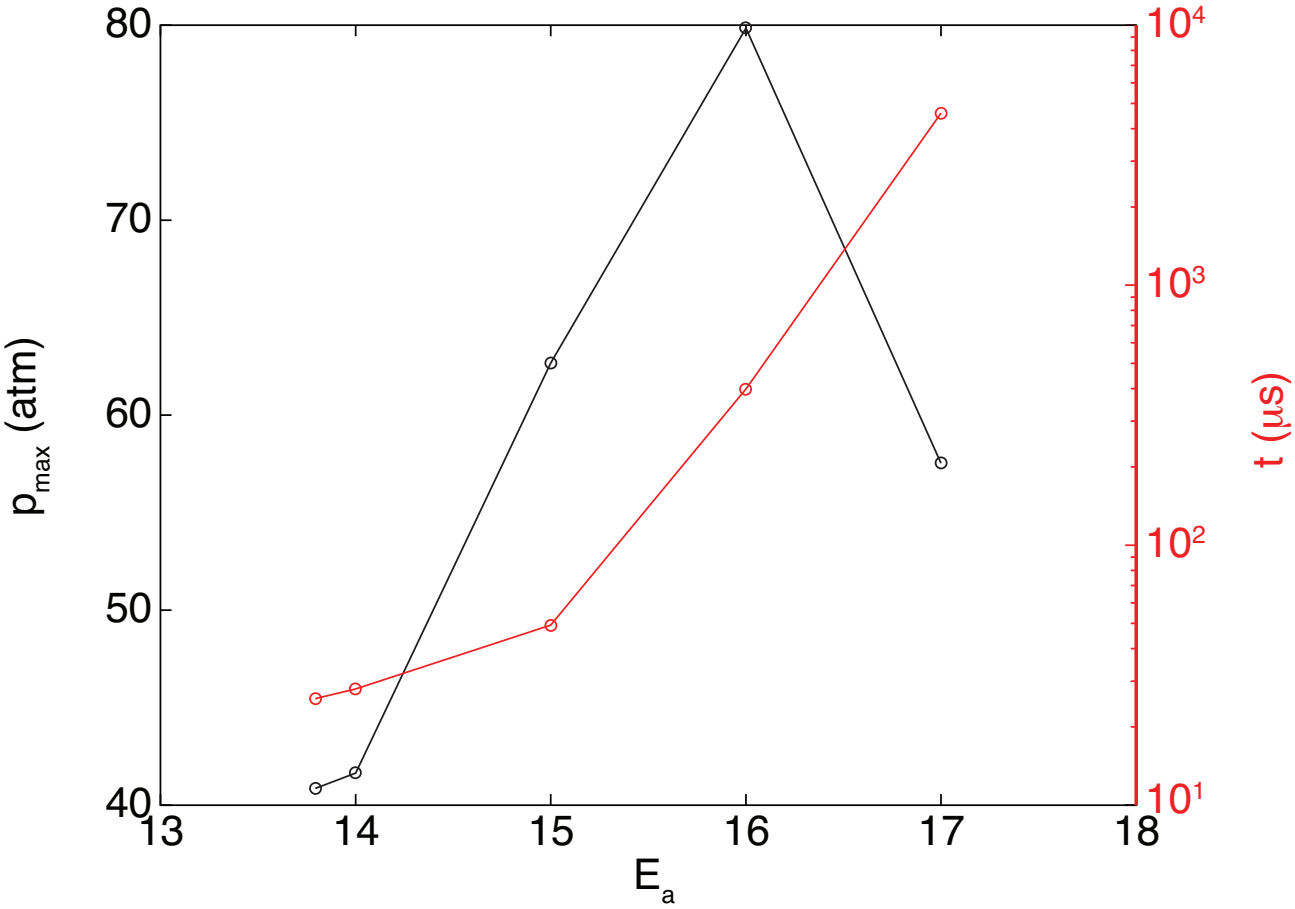

A dramatic increase in the time to detonation occurs, with a 164 times increase from $E_a = 14$ to $E_a = 17$.

Viscous Initiation - $E_a = 13.8$

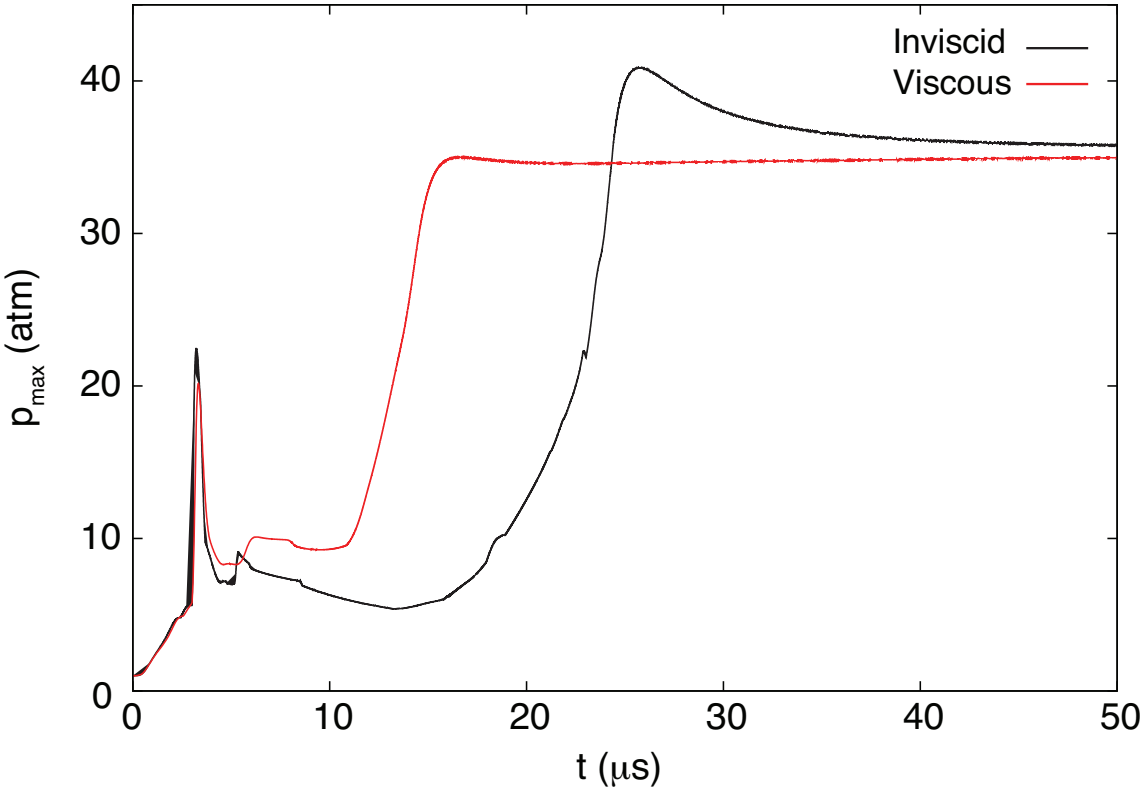

A viscosity of $2 \times 10^{-2}\ Ns/m^2$ was used to give an upper bound on the effect of diffusion, likewise the mass diffusion coefficient and thermal conductivity were set such that $L_\mu \sim L_k \sim L_\mathcal{D}$. The inviscid peak pressure of $40.9\ atm$ occurs at $25.7\ \mu s$ and the viscous analog's peak pressure of $35.0\ atm$ occurs at $16.7\ \mu s$.

Viscous Initiation - Overview

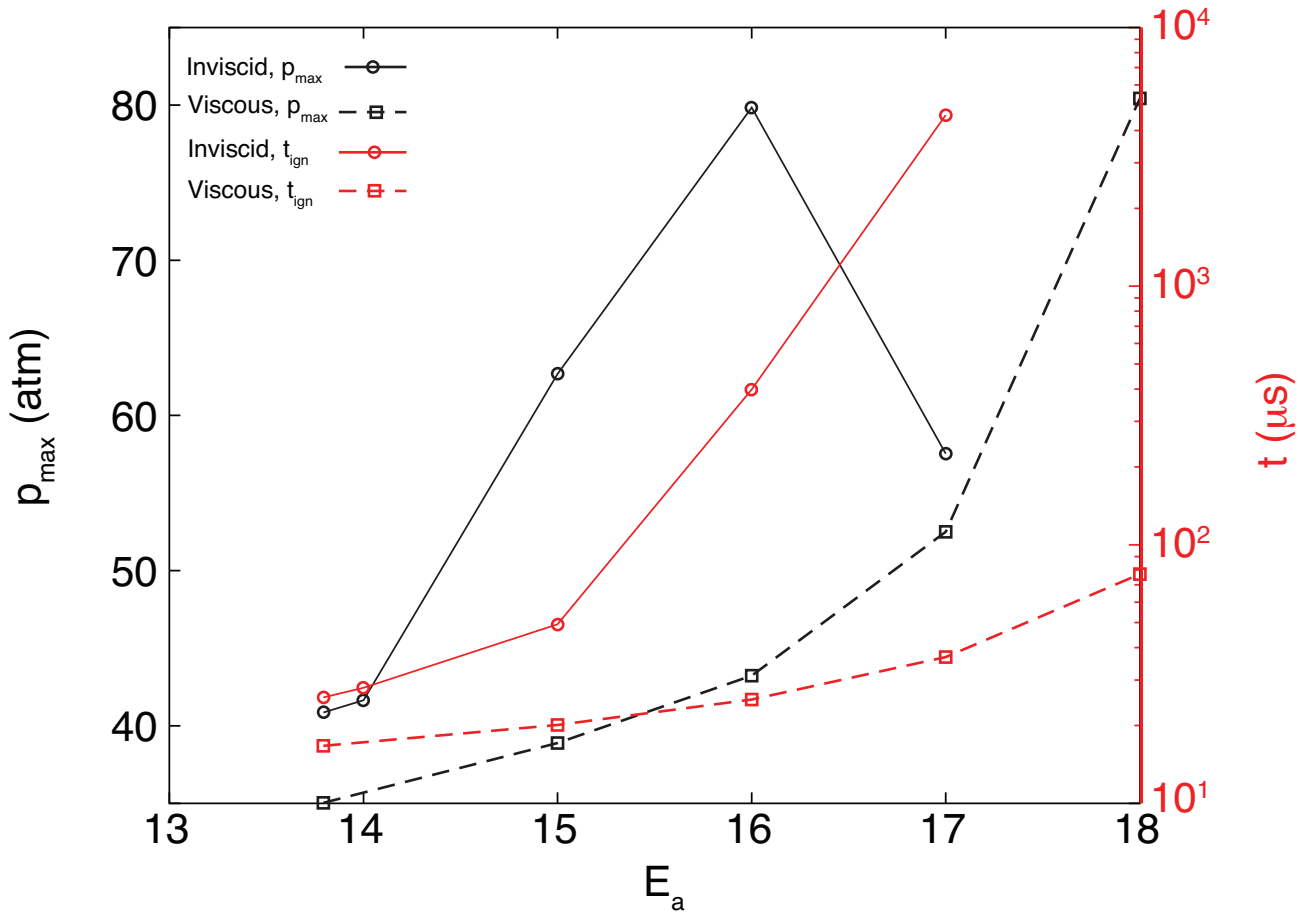

At $E_a = 17$ the viscosity induces a reduction in the time to detonation by a factor of 60.

Effect of Reducing Viscosity - $E_a = 17$

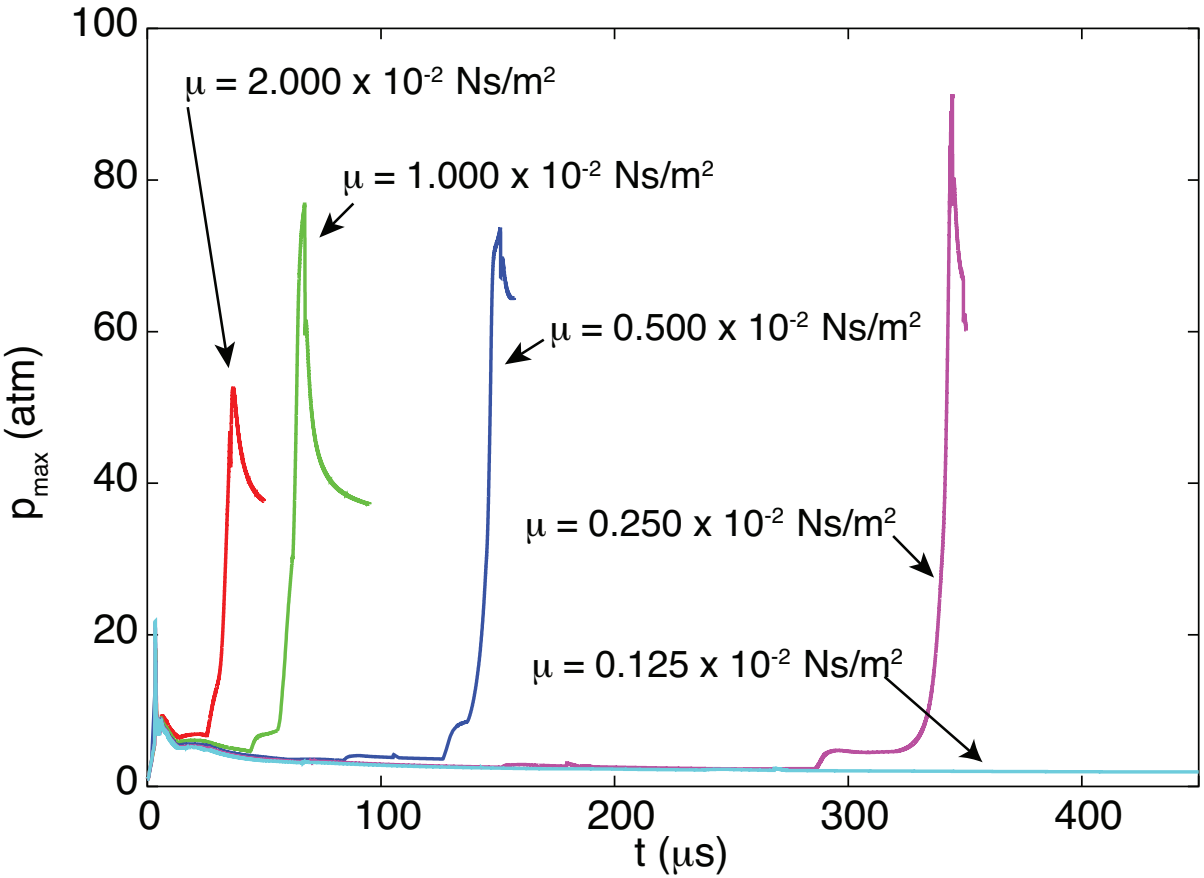

As the viscosity is reduced towards more realistic values, the time to detonation continues to increase towards the the inviscid limit.

Inviscid CJ Detonations - Parameter Set # 3

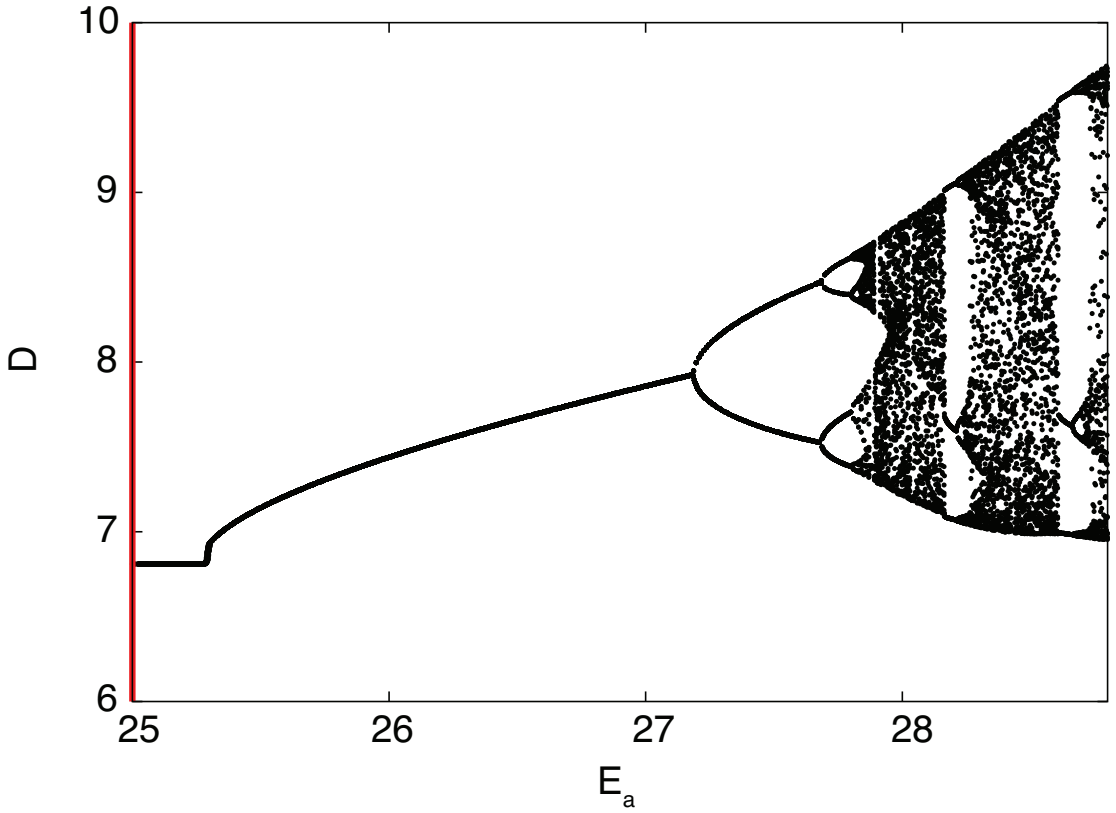

Lee & Stewart (*JFM*, 1990), Bourlioux et al. (*SIAM J. App. Math.*, 1991), Sharpe & Falle (*CTM*, 2000), Kasimov & Stewart (*Phys. Fluids*, 2004), Ng et al. (*CTM*, 2005), and Henrick et al. (*JCP*, 2006) as well as others have given insight into the behavior of inviscid planar CJ detonation waves.

Inviscid CJ - $E_a = 25$

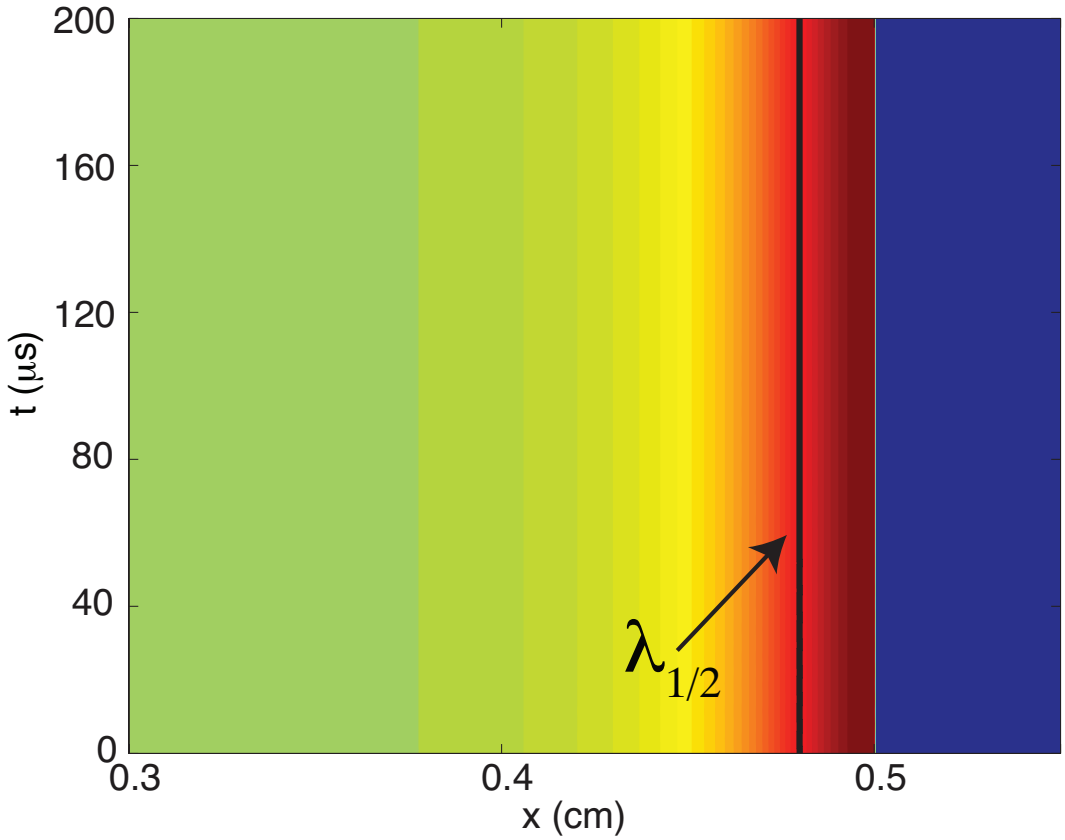

Below the neutral stability boundary, a stable, steadily propagating wave develops with $L_{1/2}$ relaxing to a constant distance behind the shock front.

Overview

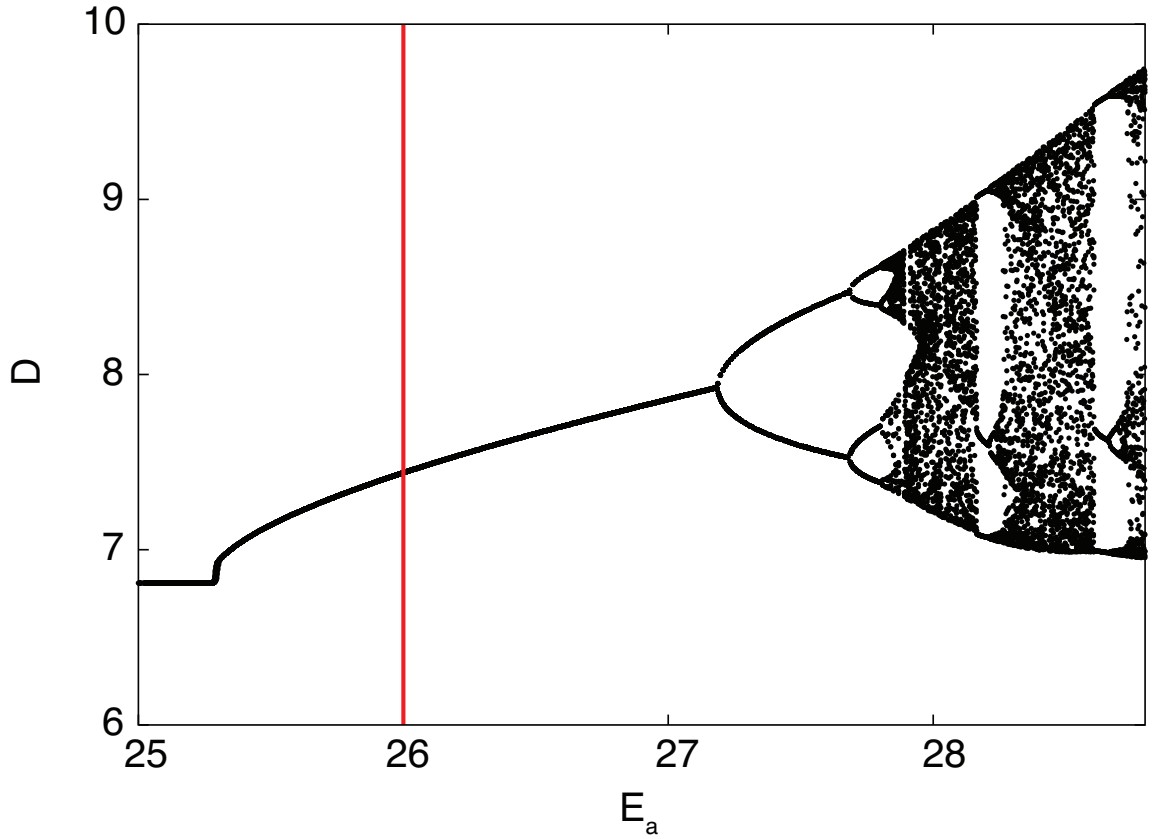

Inviscid CJ - $E_a = 26$

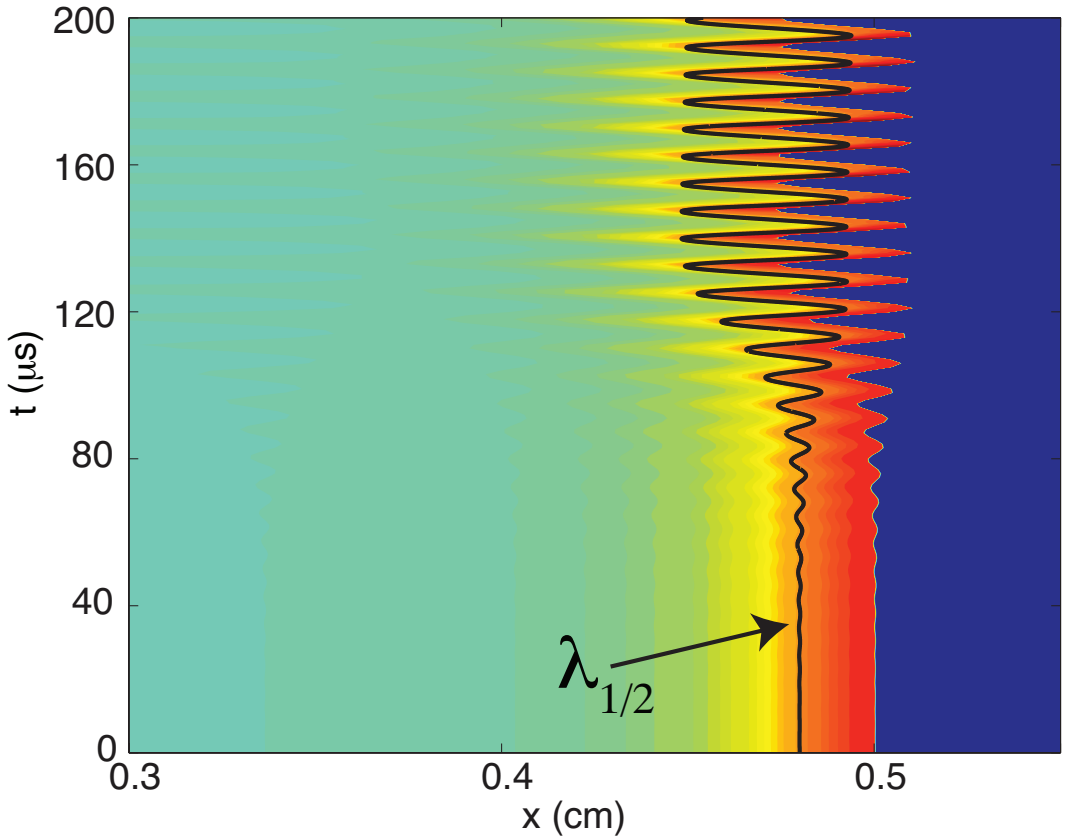

Above $E_{a_{cr}} = 25.26$, the detonation front becomes unstable, and gives rise to a minimum reaction zone length of $L_{1/2_{min}} = 1.33 \times 10^{-2}\ cm$ and $L_{1/2_{max}} = 2.71 \times 10^{-2}\ cm$ yielding $L_{1/2_{max}}/L_{1/2_{min}} = 2.04$.

Overview

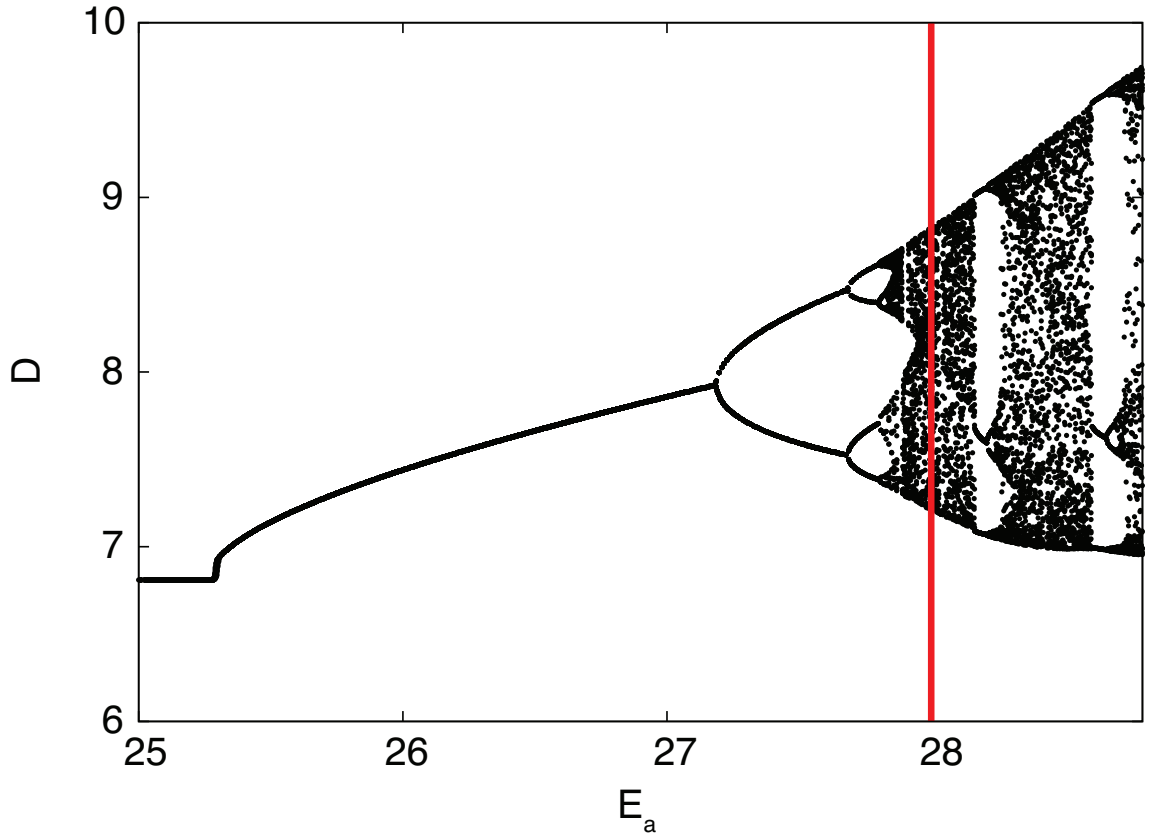

Inviscid CJ - $E_a = 28$

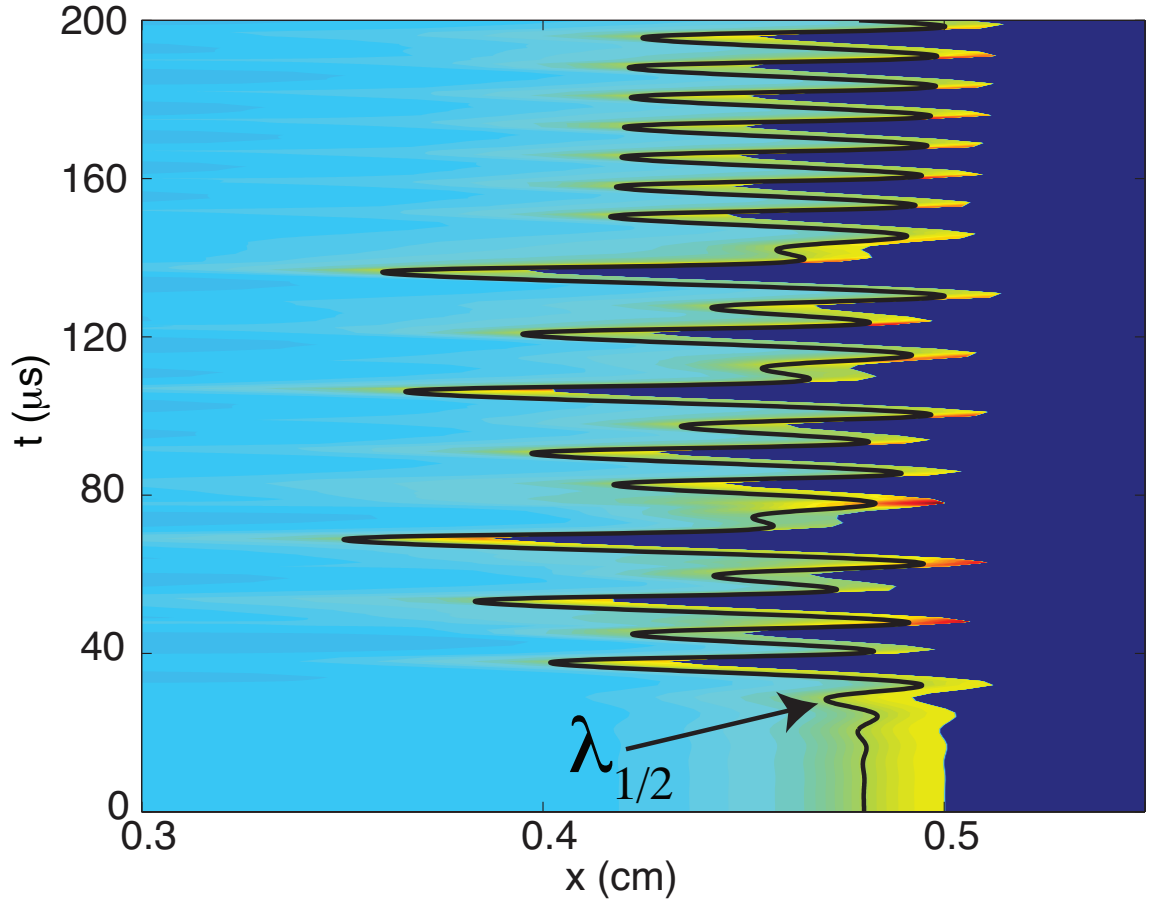

This activation energy yields a chaotic detonation, and the ratio of $L_{1/2_{max}}/L_{1/2_{min}}$ becomes 7.29.

Overview

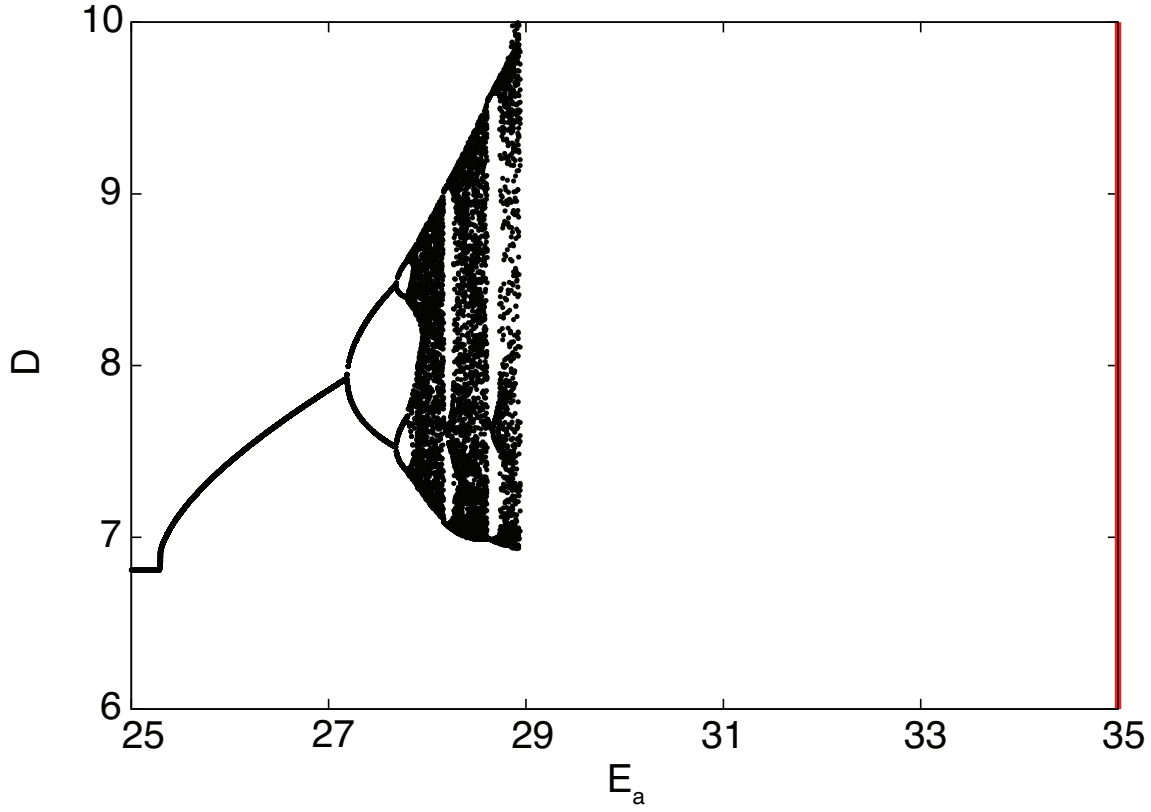

Let us examine a higher activation energy that is more representative of a hydrogen-air mixture where shock-capturing must be used.

Inviscid CJ - $E_a = 35$

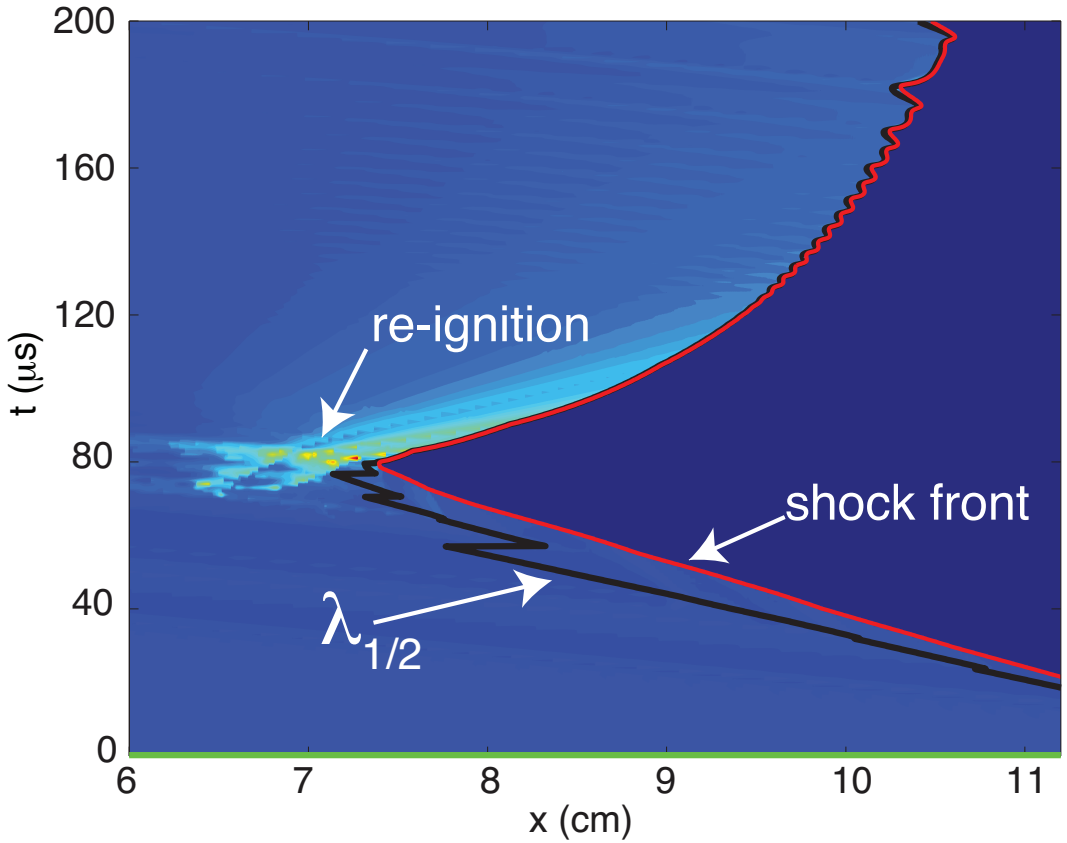

The detonation fails initially, leading to the formation of a weakened leading shock, contact discontinuity, and a rarefaction wave to the CJ state, before an eventual re-ignition.

ZND Profile

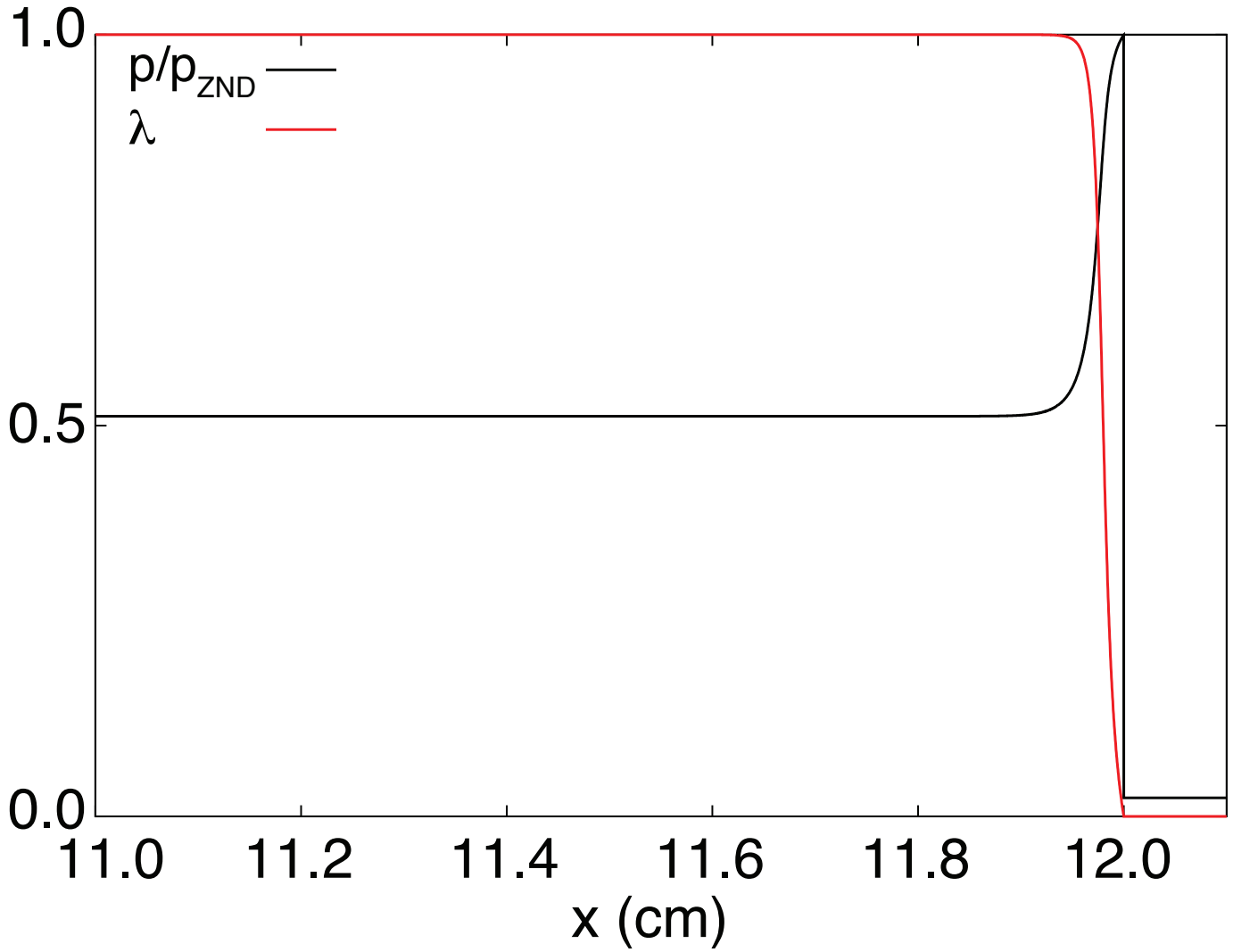

Inviscid CJ - $E_a = 35$

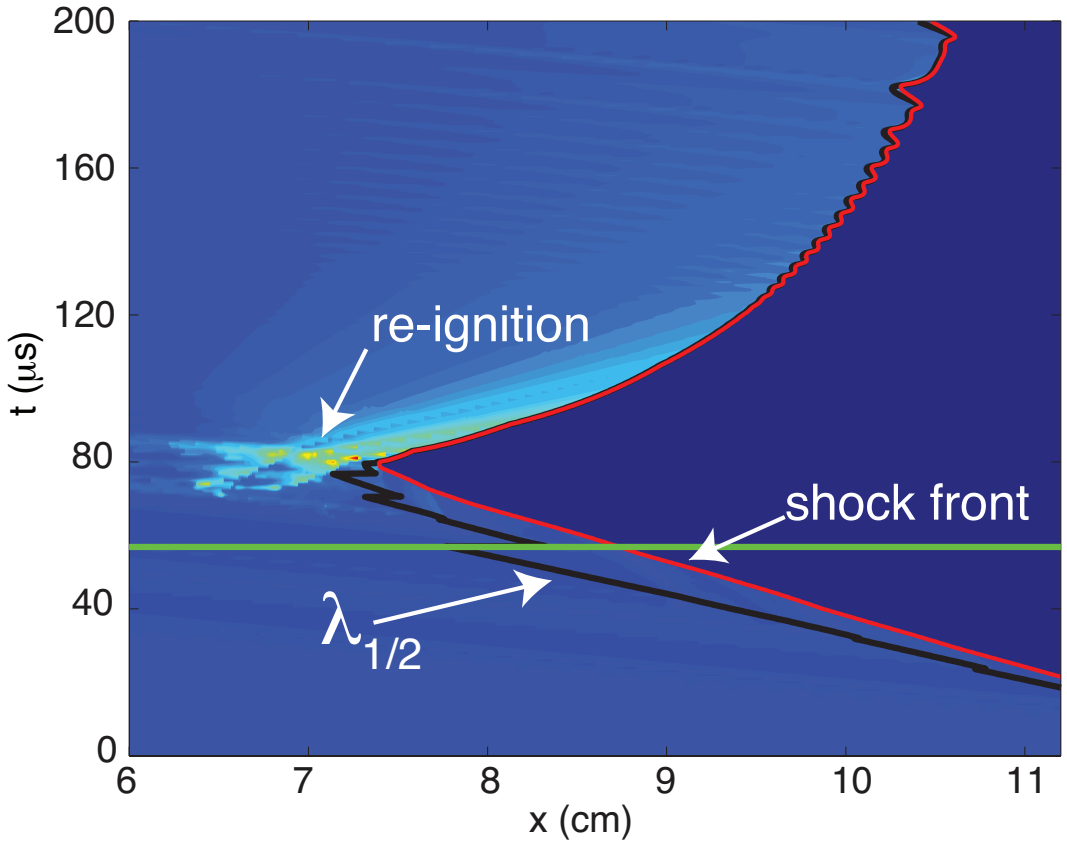

The detonation fails initially, leading to the formation of a weakened leading shock, contact discontinuity, and a rarefaction wave to the CJ state, before an eventual re-ignition.

Profile After Failure

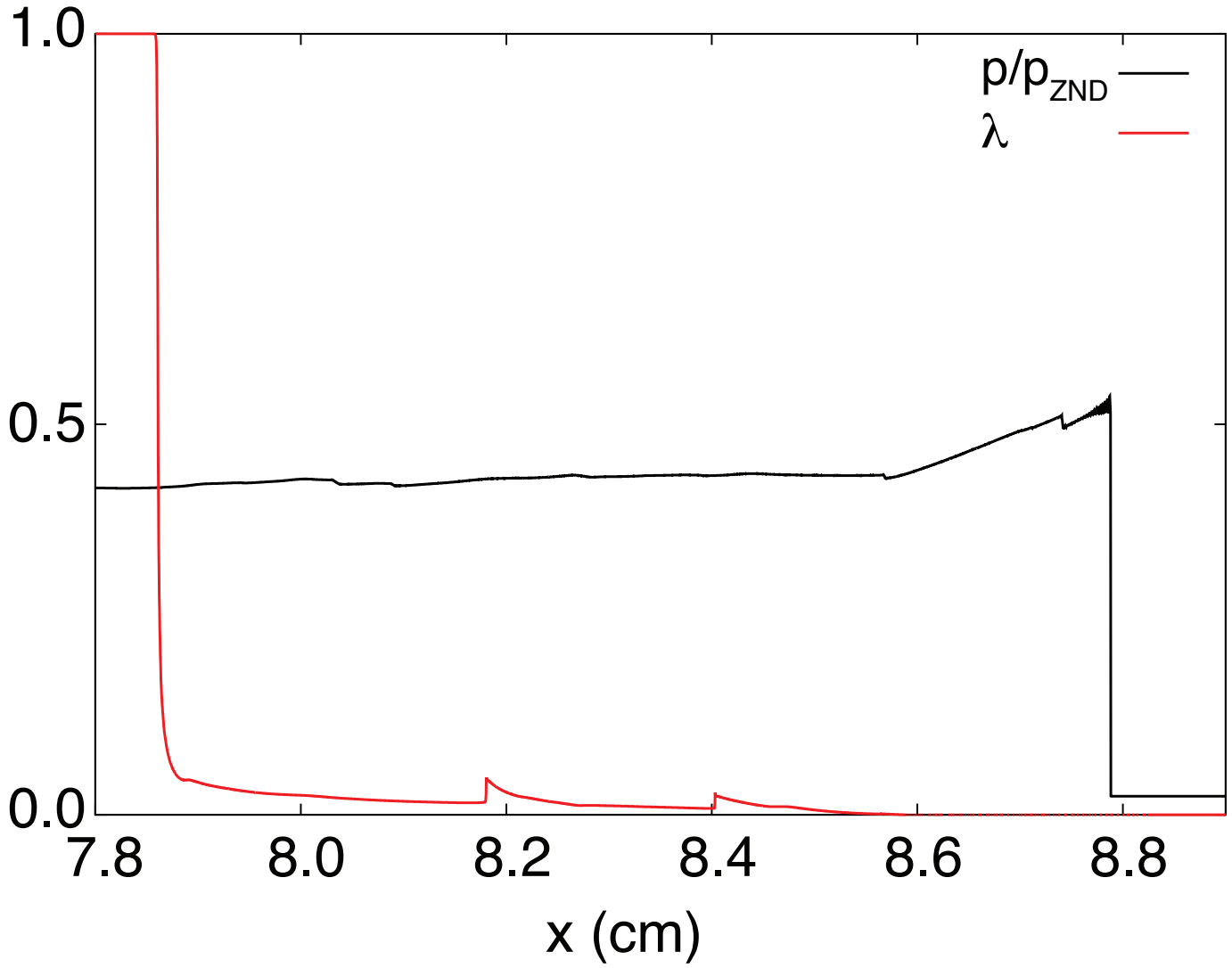

Inviscid CJ - $E_a = 35$

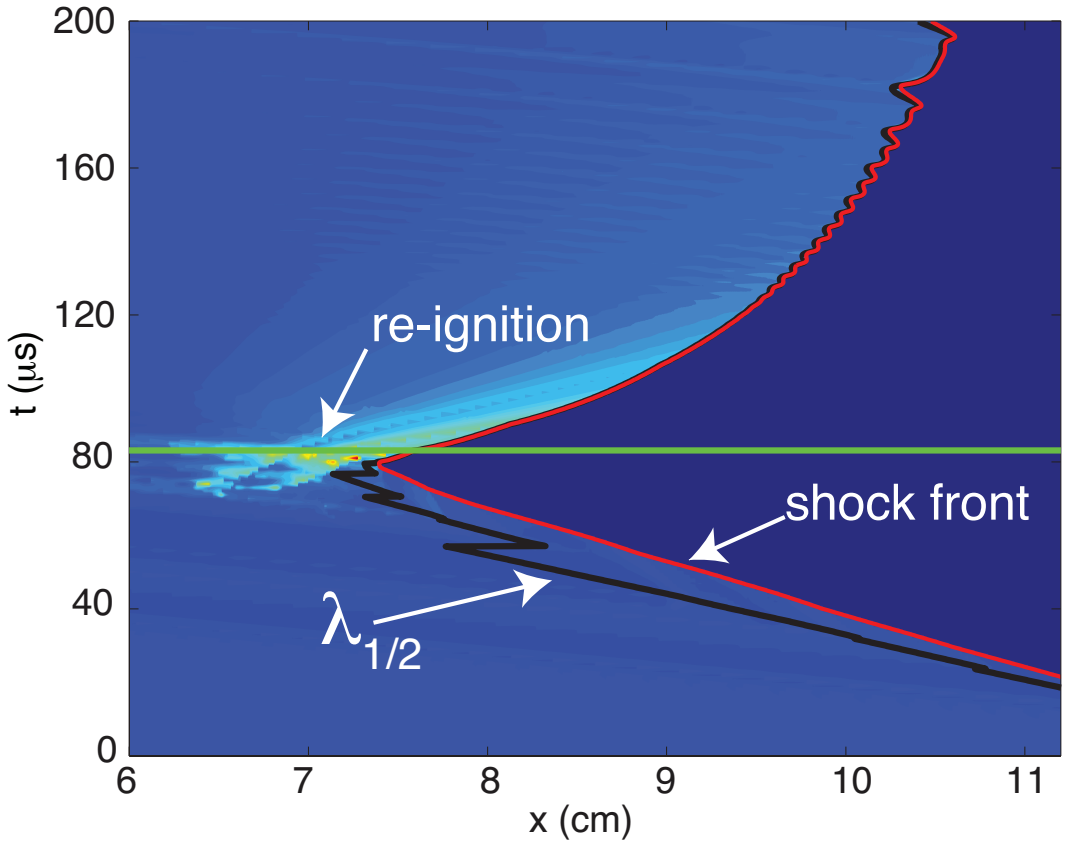

The detonation fails initially, leading to the formation of a weakened leading shock, contact discontinuity, and a rarefaction wave to the CJ state, before an eventual re-ignition.

Profile After Re-ignition

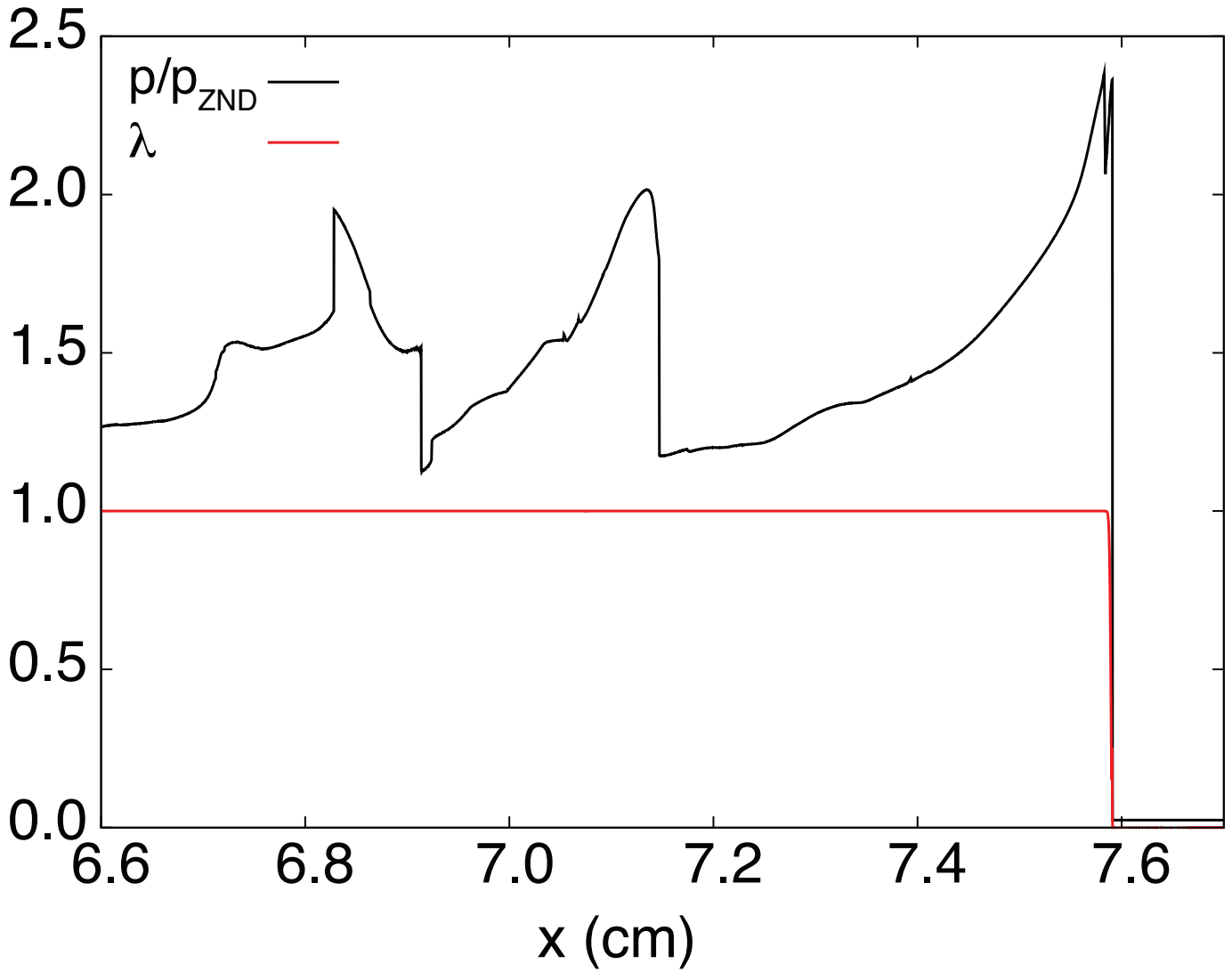

Longest Length Scale Estimate

- Solve Riemann problem from ambient conditions and CJ conditions
- Assume inertial confinement (adiabatic, isochoric thermal auto-ignition) behind the leading weakened shock:

$$\frac{\partial \lambda}{\partial t} = a\left(1-\lambda\right)\exp\left(\frac{-E_a}{\left(p/\rho\right)}\right),$$

$$\frac{p}{\left(\gamma-1\right)\rho} - q\lambda = C$$

- This yields an auto-ignition time and distance of:

$$t_{ign} = \int_0^{1/2} \frac{1}{a\left(1-\lambda\right)\exp\left(\frac{-E_a}{\left(p_s/\rho_s+(\gamma-1)q\lambda\right)}\right)} d\lambda,$$

$$L_{ign} = (D_s - u_s)t_{ign}$$

- The kinetic rate constant, a, is maintained such that $L_{1/2} = 2 \times 10^{-2}\ cm$ for the steady $CJ\text{-}ZND$ profile

Shortest Length Scale Estimate

- After re-ignition, the detonation becomes strongly overdriven
- At a high enough overdrive, the shocked temperature dominates the activation energy in the chemical reaction term
- This causes the exponential in the Arrenhenius kinetics to be ~ 1
- Given that the kinetic rate constant, a, is maintained such that the steady $L_{1/2} = 2 \times 10^{-2}\ cm$, there is a specific overdrive at which the interaction between the rate of chemical reaction and the post-shock velocity yields a minimum $L_{1/2}$

$L_{1/2}$ Variation

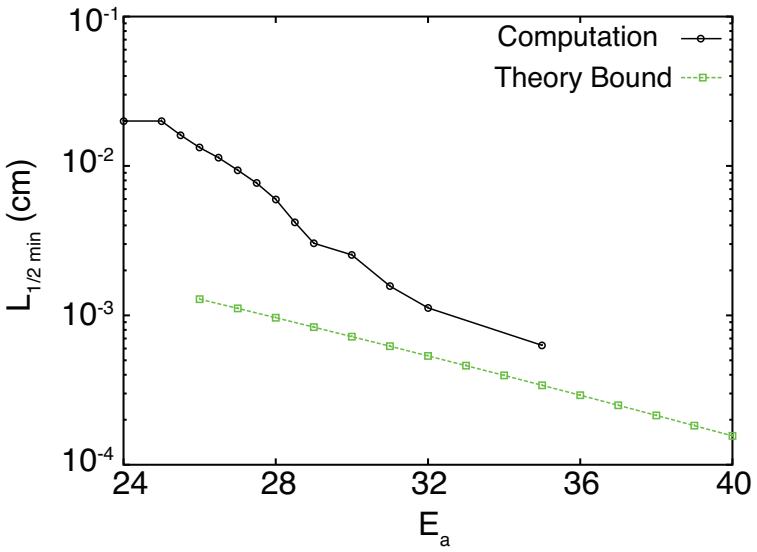

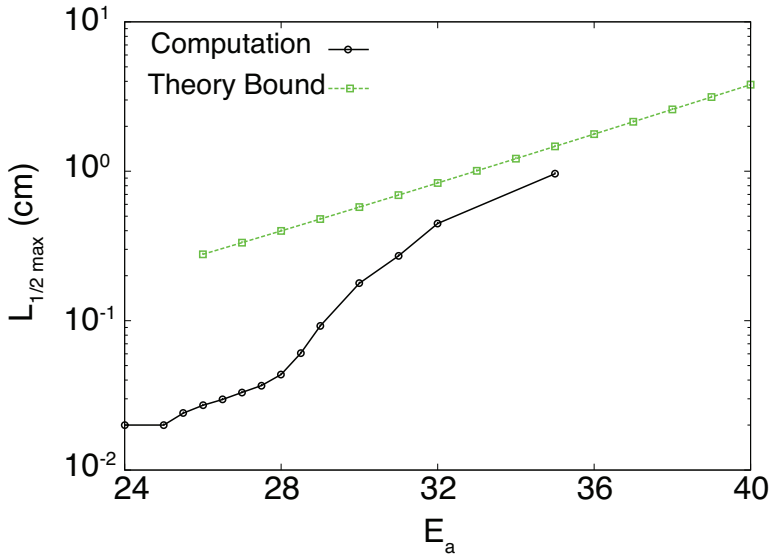

Once the detonation becomes unstable, the minimum $L_{1/2}$ decreases and the maximum $L_{1/2}$ increases as activation energy increases.

$L_{1/2}$ Ratio - Inviscid

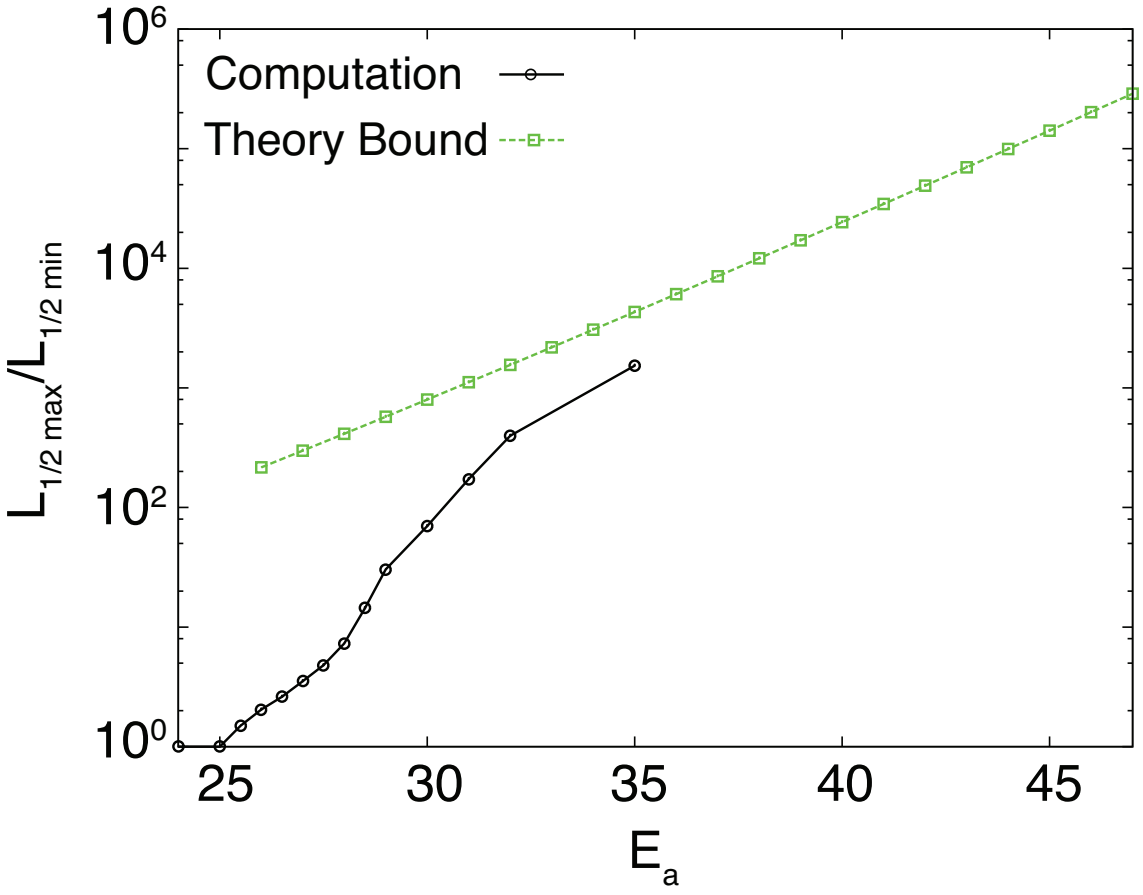

Once the detonation becomes unstable, the $L_{1/2}$ ratio shows a power law growth before approaching the upper bound estimate as the activation energy increases.

$L_{1/2}$ Ratio - Inviscid

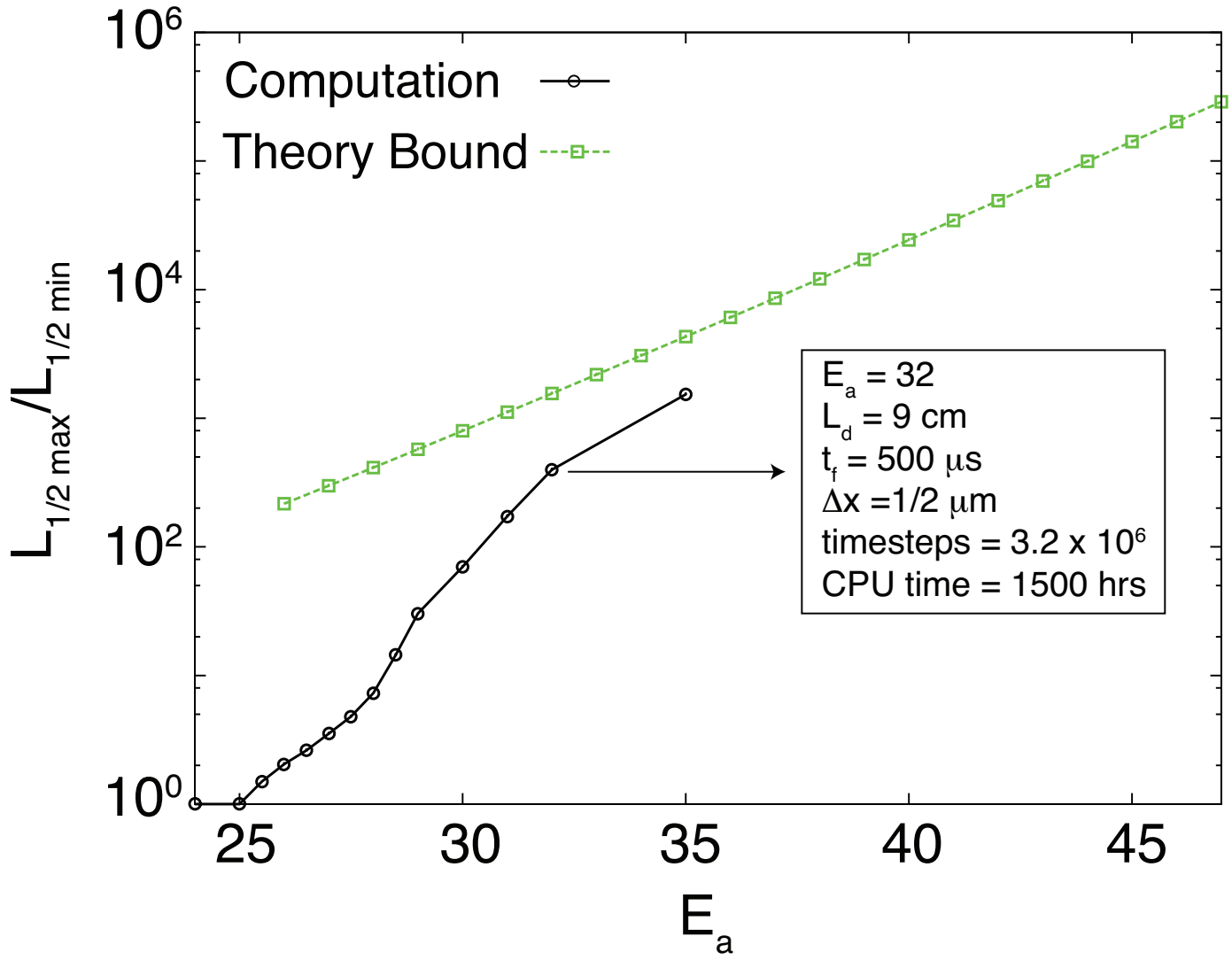

$L_{1/2}$ Ratio - Inviscid

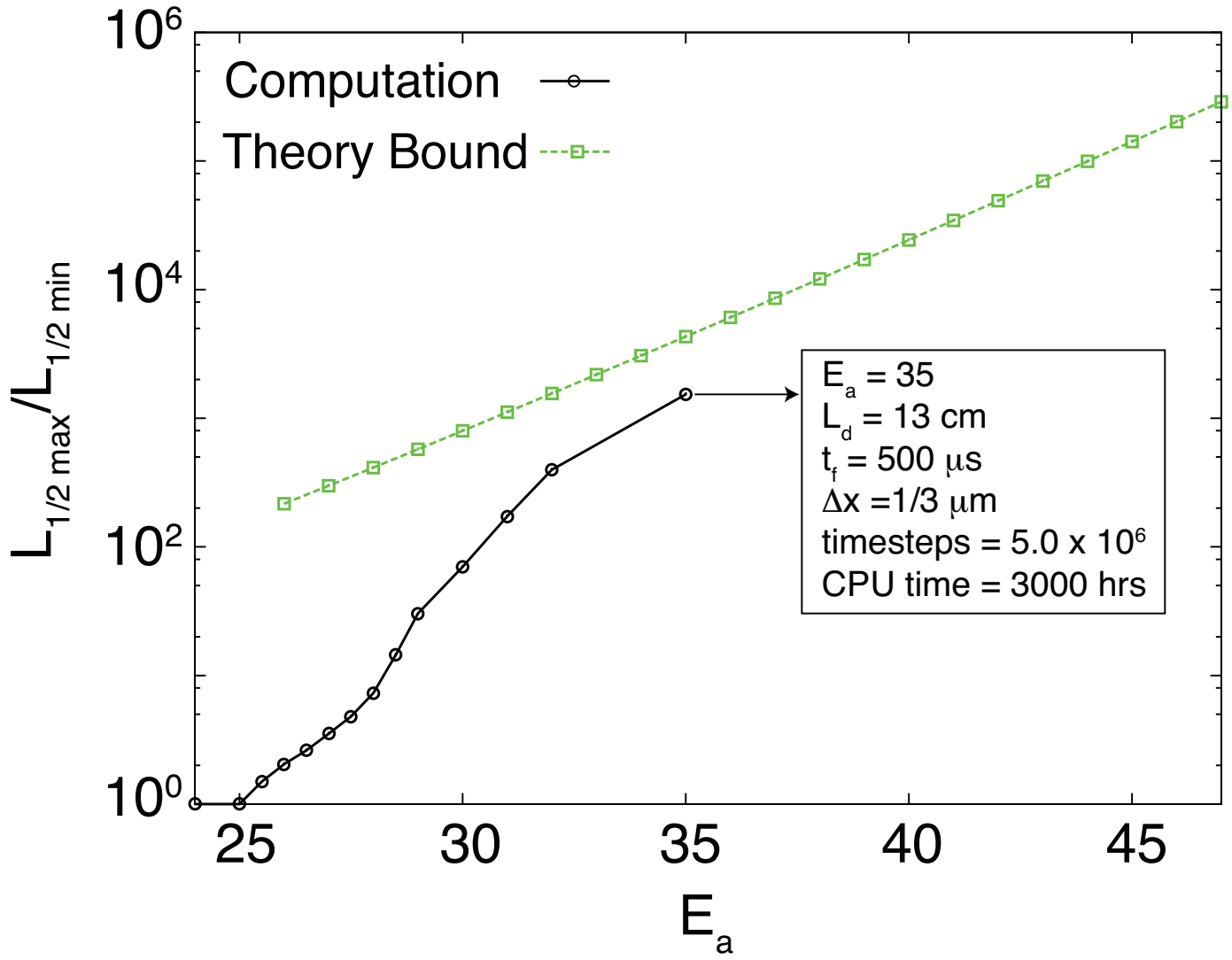

$L_{1/2}$ Ratio - Inviscid

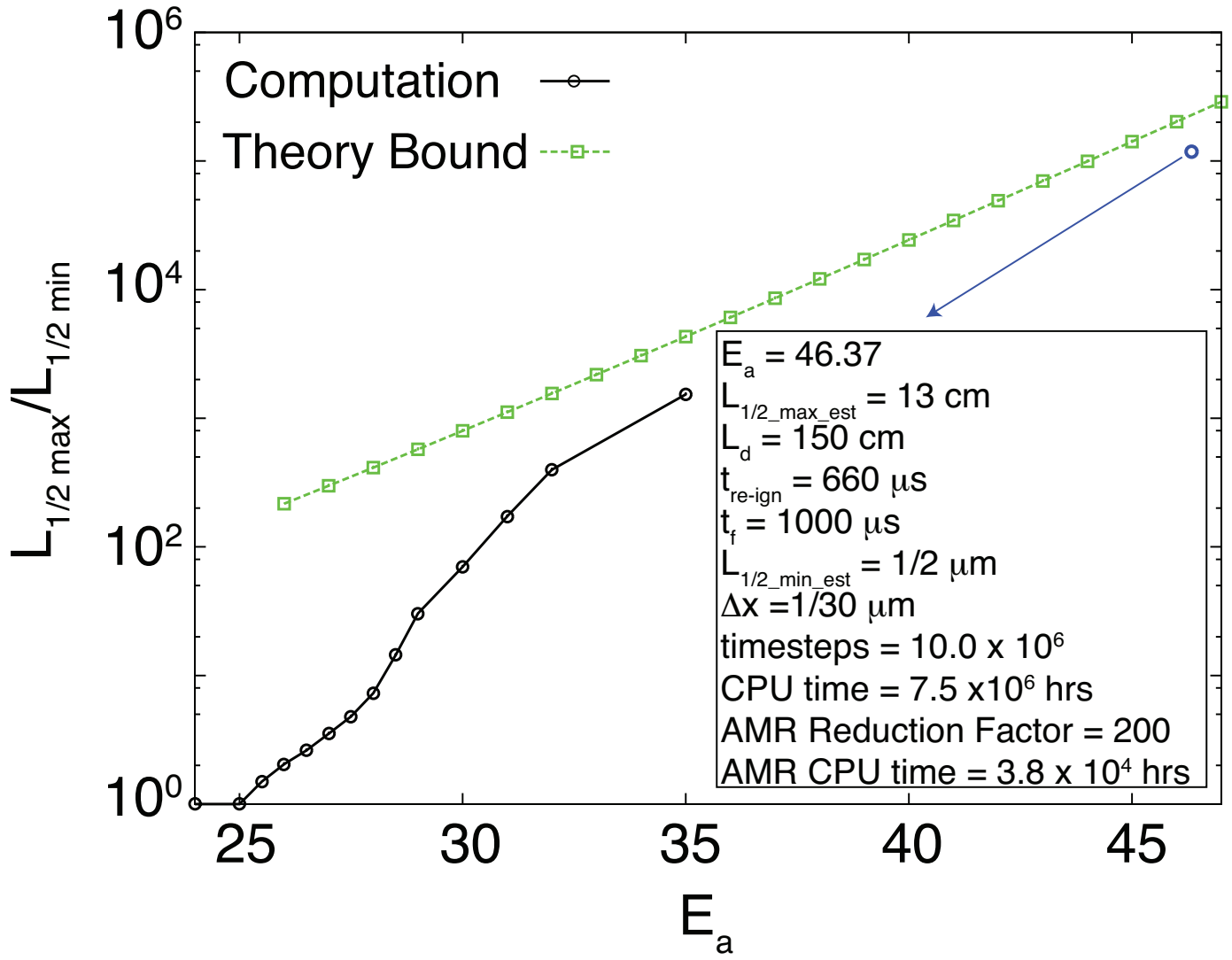

Viscous CJ - $E_a = 26$

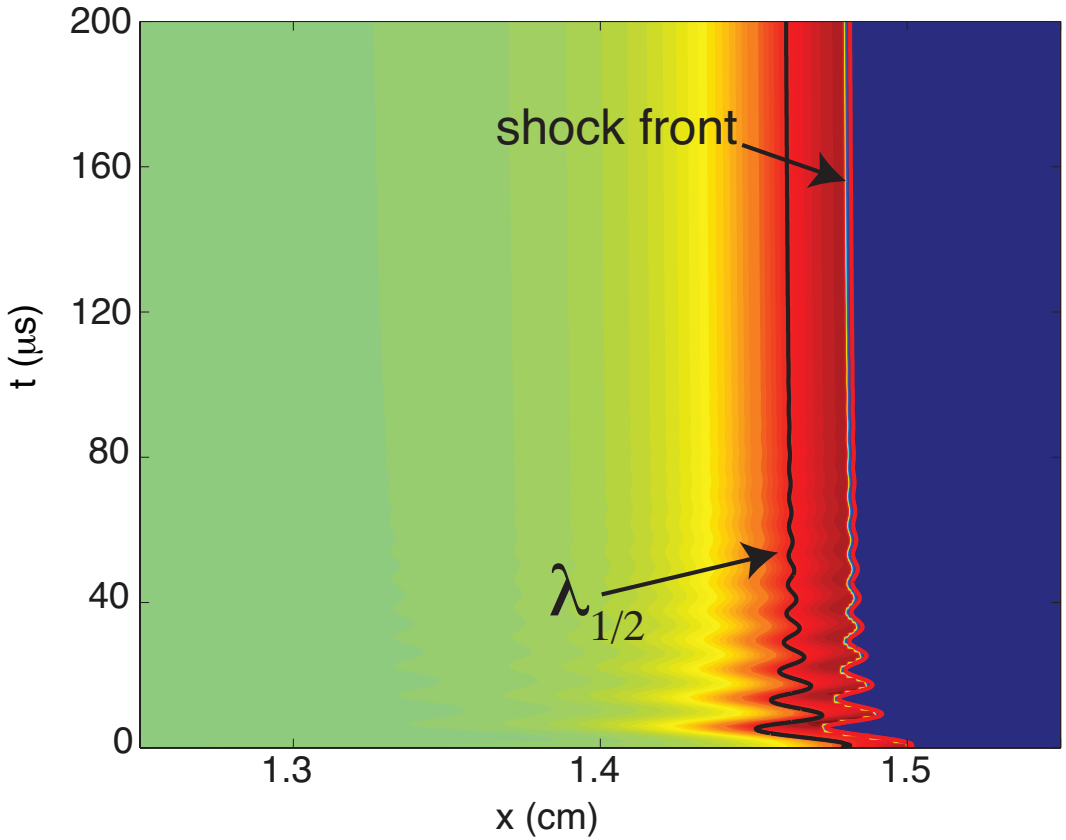

By adding $\mu = 2 \times 10^{-2}\ Ns/m^2$, we obtain an upper bound on the effect of diffusion on the propagation, similar to the initiation. At this activation energy, a stable detonation forms yielding a constant $L_{1/2}$ at long times.

Viscous CJ - $E_a = 28$

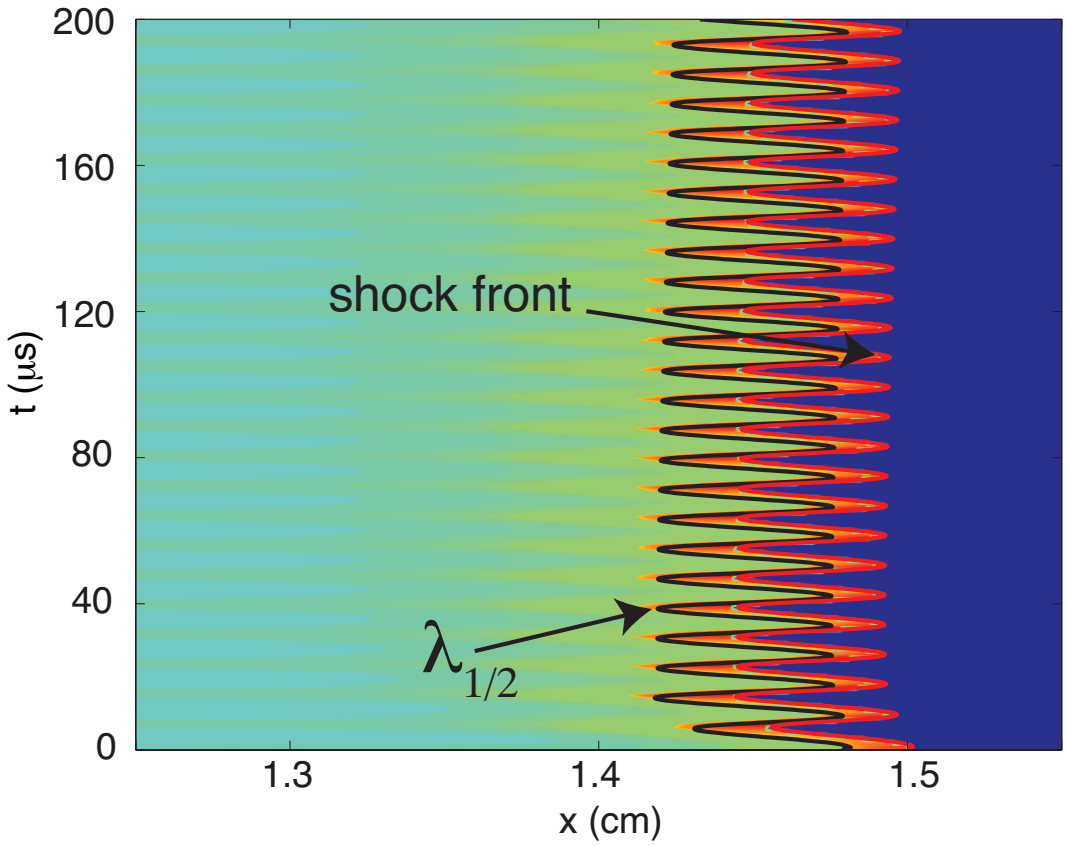

Even with viscosity, a high enough activation energy gives rise to an unstable detonation. For this period-1 detonation, the ratio $L_{1/2_{max}}/L_{1/2_{min}} = 2.53.$

Viscous CJ - $E_a = 33$

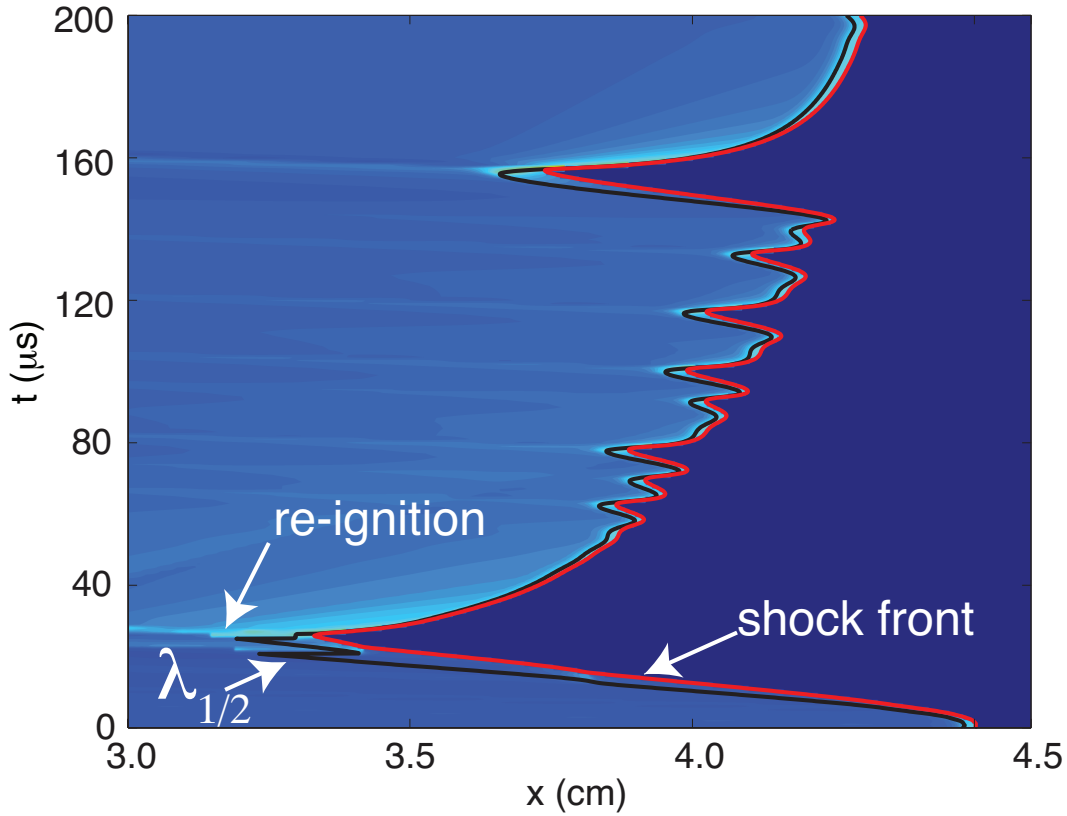

Similar to that predicted in the inviscid limit, at activation energies more representative of a hydrogen-air mixture, the detonation fails initially. In this case, the ratio of $L_{1/2_{max}}/L_{1/2_{min}}$ grows to 224.

$L_{1/2}$ Ratio - Viscous

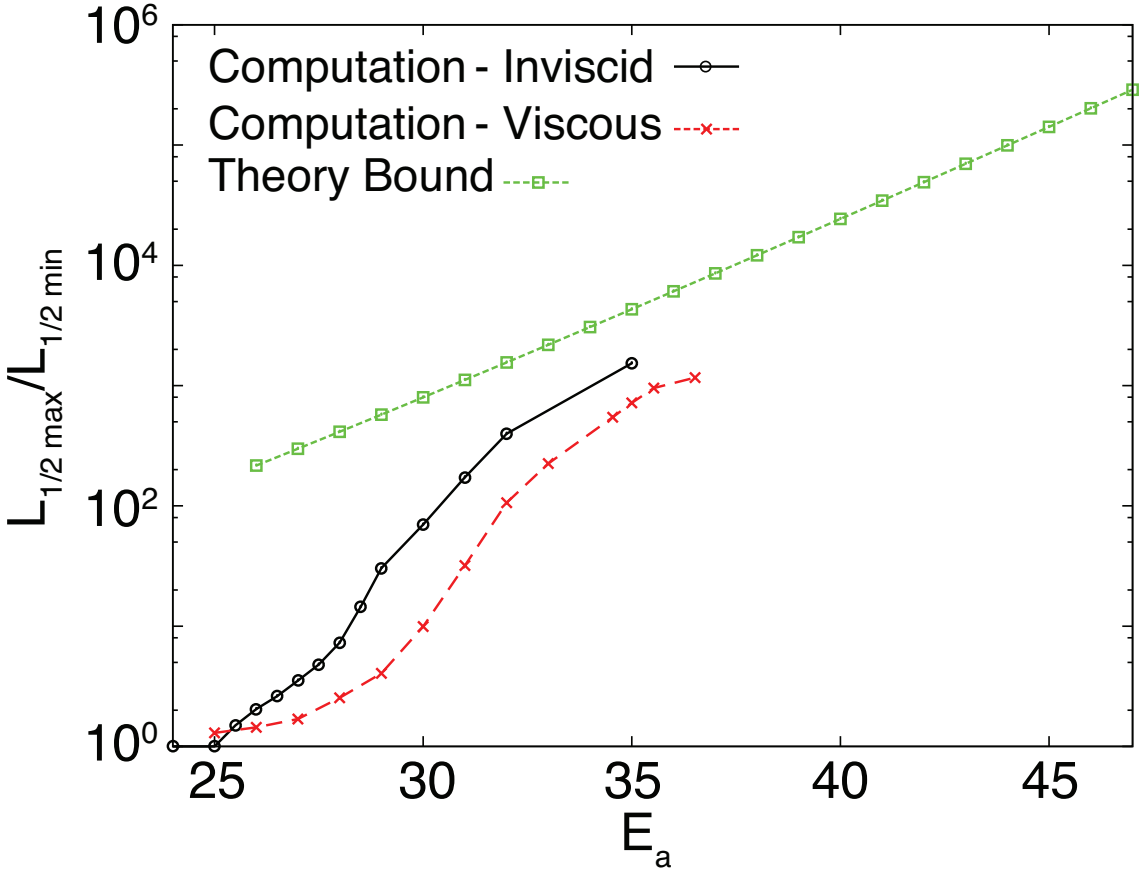

The addition of diffusion causes a shift in the neutral stability, and thus reduces the ratio of $L_{1/2}$ at a given activation energy.

$L_{1/2}$ Ratio - Viscous

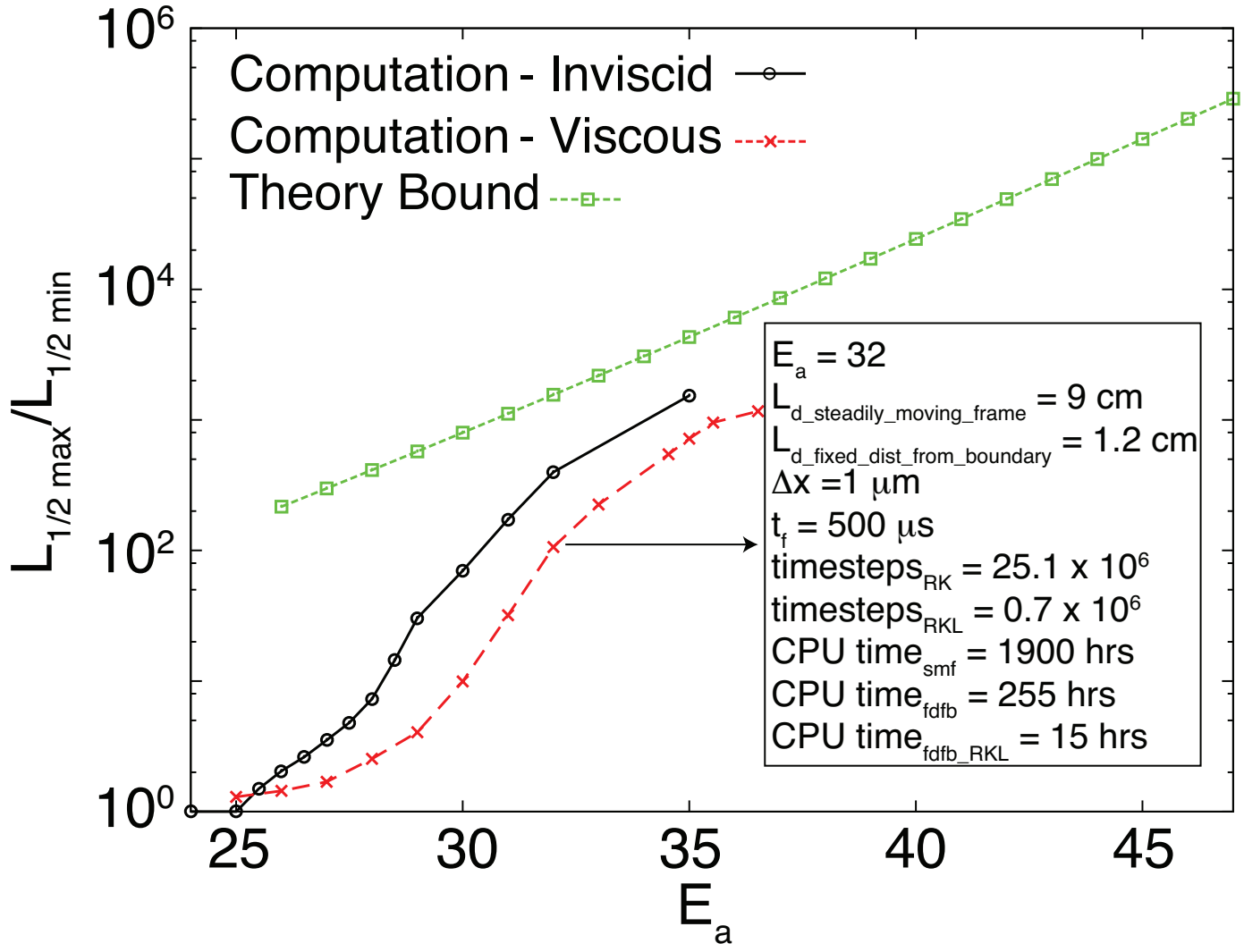

$L_{1/2}$ Ratio - Viscous

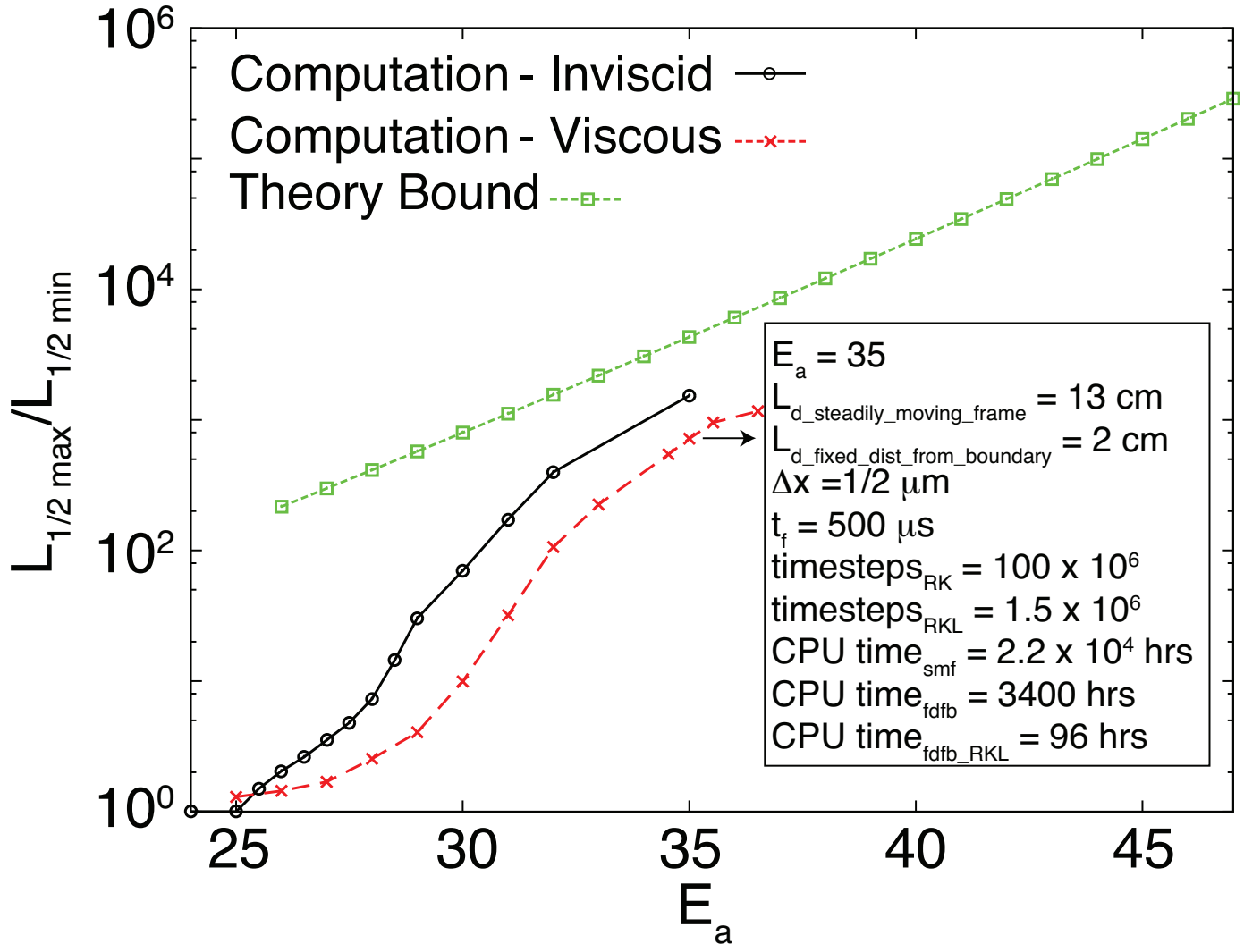

$L_{1/2}$ Ratio - Viscous

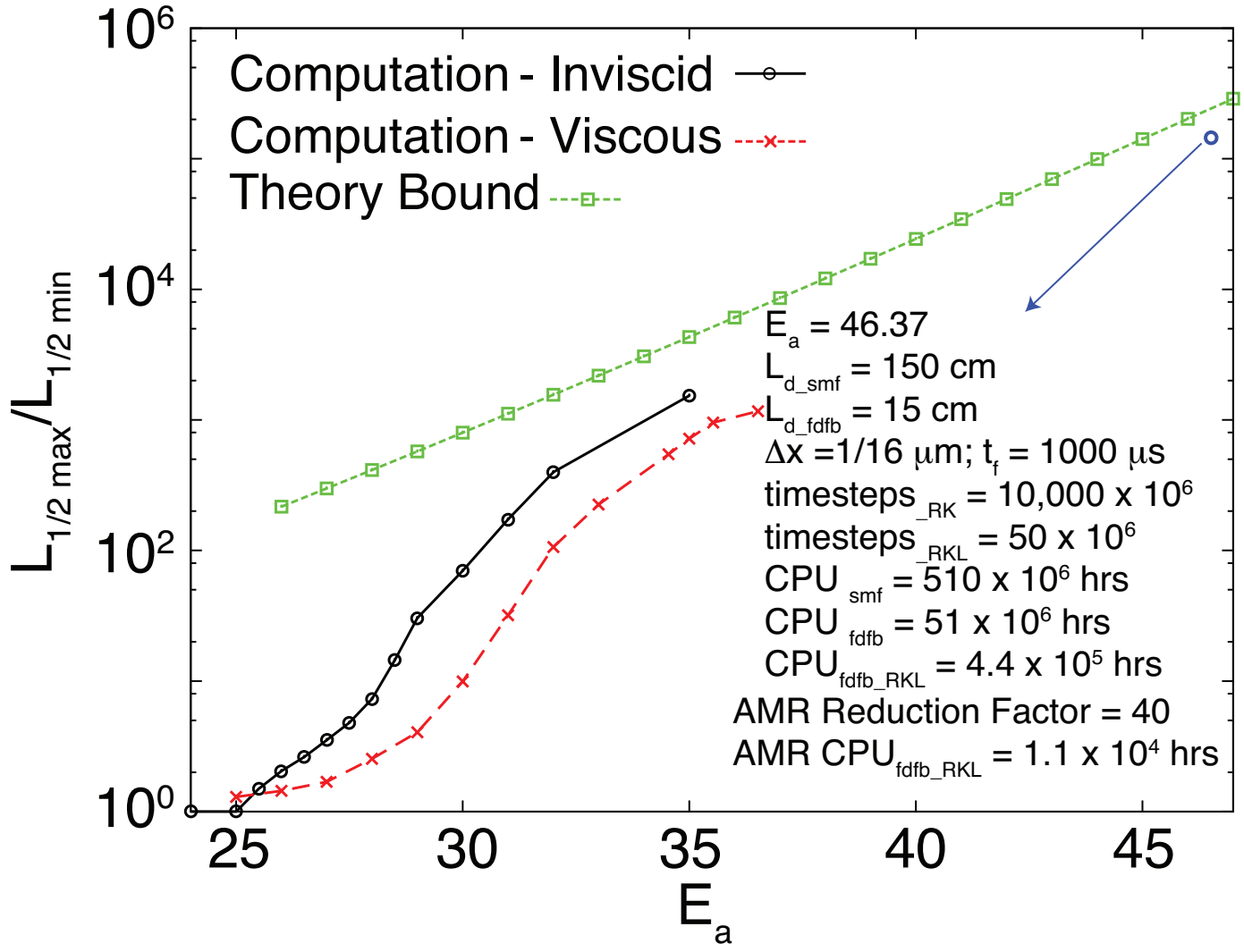

Chemical Mechanism

Having a better understanding of the length scales present in the one-step model, let's examine detailed kinetics using the parameter of overdrive.

j	Reaction	a_j	β_j	E_j
1	$H_2 + O_2 \rightleftharpoons 2OH$	1.70×10^{13}	0.00	47780
2	$OH + H_2 \rightleftharpoons H_2O + H$	1.17×10^{9}	1.30	3626
3	$H + O_2 \rightleftharpoons OH + O$	5.13×10^{16}	−0.816	16507
4	$O + H_2 \rightleftharpoons OH + H$	1.80×10^{10}	1.00	8826
5	$H + O_2 + M \rightleftharpoons HO_2 + M^a$	2.10×10^{18}	−1.00	0
6	$H + O_2 + O_2 \rightleftharpoons HO_2 + O_2$	6.70×10^{19}	−1.42	0
7	$H + O_2 + N_2 \rightleftharpoons HO_2 + N_2$	6.70×10^{19}	−1.42	0
8	$OH + HO_2 \rightleftharpoons H_2O + O_2$	5.00×10^{13}	0.00	1000
9	$H + HO_2 \rightleftharpoons 2OH$	2.50×10^{14}	0.00	1900
10	$O + HO_2 \rightleftharpoons O_2 + OH$	4.80×10^{13}	0.00	100
11	$2OH \rightleftharpoons O + H_2O$	6.00×10^{8}	1.30	0
12	$H_2 + M \rightleftharpoons H + H + M^b$	2.23×10^{12}	0.50	92600
13	$O_2 + M \rightleftharpoons O + O + M$	1.85×10^{11}	0.50	95560
14	$H + OH + M \rightleftharpoons H_2O + M^c$	7.50×10^{23}	−2.60	0
15	$H + HO_2 \rightleftharpoons H_2 + O_2$	2.50×10^{13}	0.00	700
16	$HO_2 + HO_2 \rightleftharpoons H_2O_2 + O_2$	2.00×10^{12}	0.00	0
17	$H_2O_2 + M \rightleftharpoons OH + OH + M$	1.30×10^{17}	0.00	45500
18	$H_2O_2 + H \rightleftharpoons HO_2 + H_2$	1.60×10^{12}	0.00	3800
19	$H_2O_2 + OH \rightleftharpoons H_2O + HO_2$	1.00×10^{13}	0.00	1800

Enhanced third-body efficiencies with M:

M^a: $f_{H_2O} = 21.0, f_{H_2} = 3.30, f_{N_2} = 0.00, f_{O_2} = 0.00$

M^b: $f_{H_2O} = 6.00, f_H = 2.00, f_{H_2} = 3.00$

M^c: $f_{H_2O} = 20.0$

Miller (*19th Symposium (International) on Combustion*, 1982)

Strongly Overdriven - Stable $(f = 1.25)$

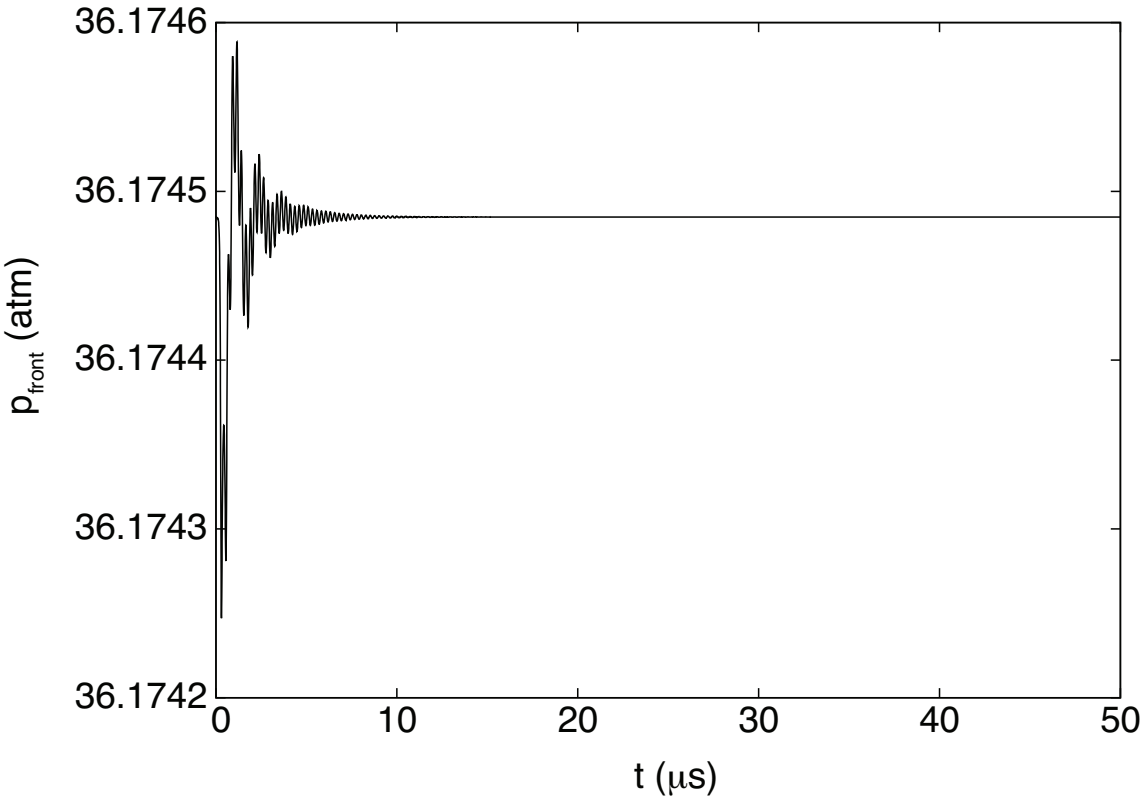

At a strong enough overdrive, a hydrogen-air detonation becomes stable, producing a steady propagating wave.

Strongly Overdriven - Stable - Length Scales

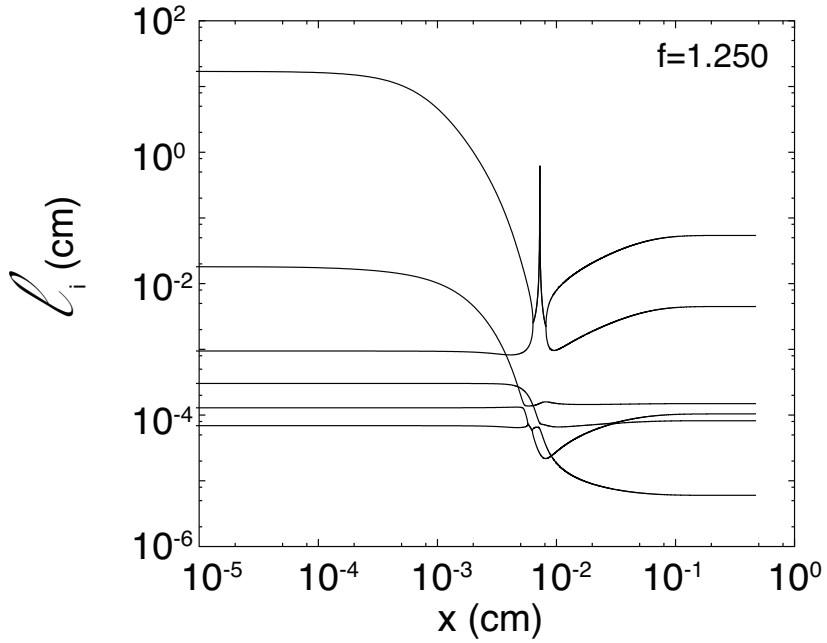

Even for a stable detonation in hydrogen-air, multiple lengths scales appear. $L_{min} = 6.0 \times 10^{-6}\ cm$ and $L_{max} = 1.7 \times 10^{1}\ cm$. This yields a ratio of $L_{max}/L_{min} = 2.8 \times 10^{6}$. The induction zone length is $7.3 \times 10^{-3}\ cm$.

Overdriven - Unstable $(f = 1.15)$

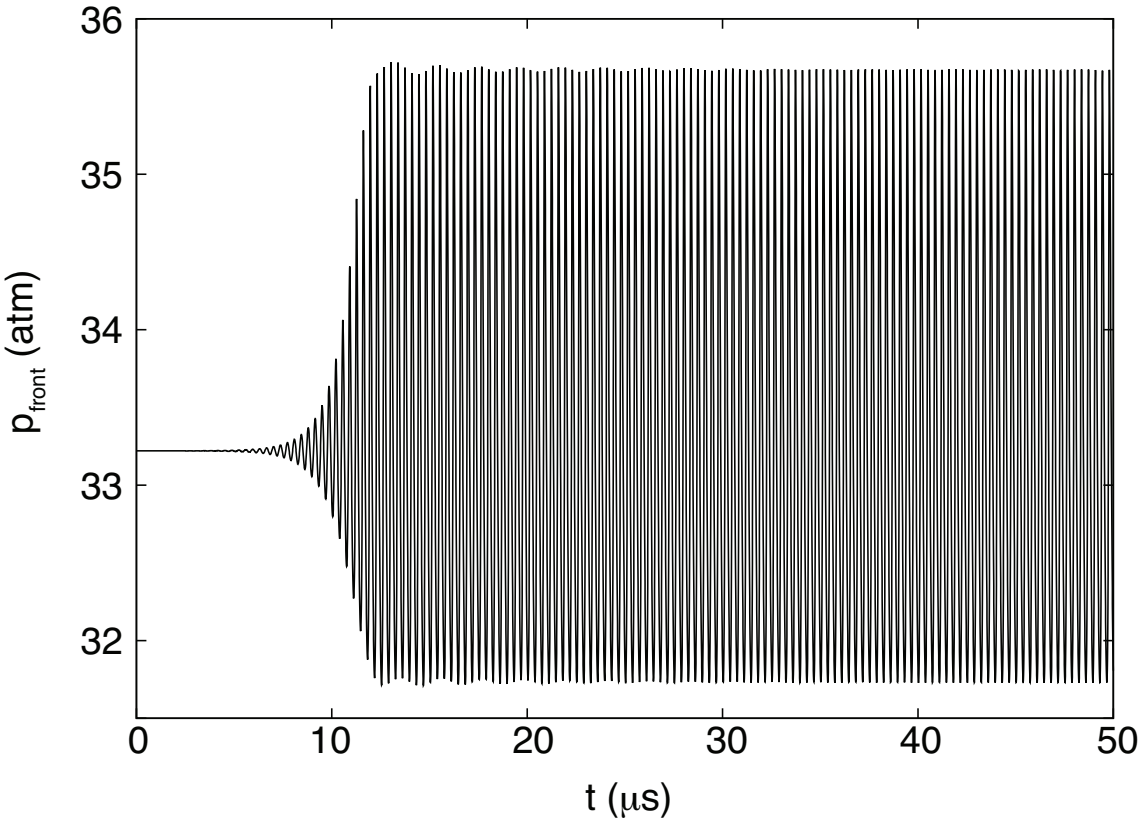

Below the neutral stability point, the ZND detonation is unstable. If a quasi-steady ZND profile is assumed at the maximum and minimum overdrives predicted, an estimate of the length scales present during the evolution can be obtained.

Overdriven - Unstable - Length Scales

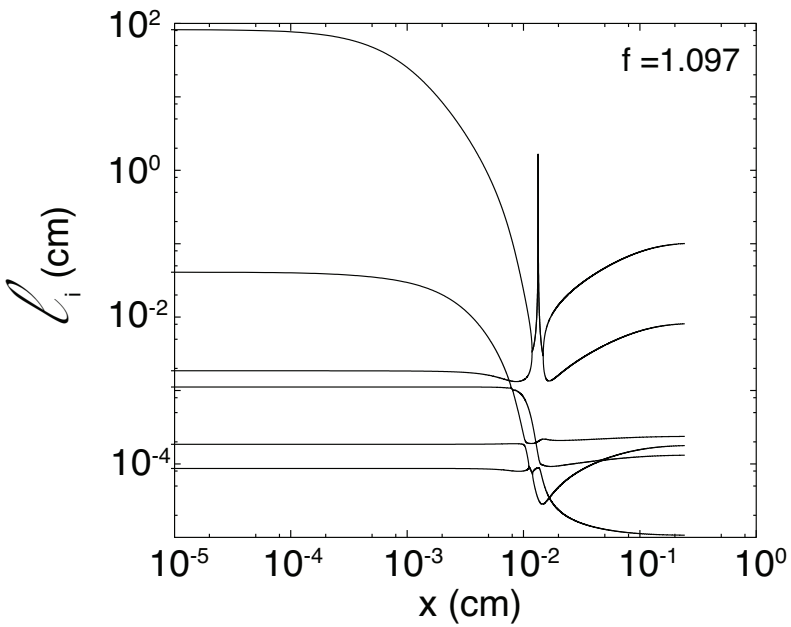

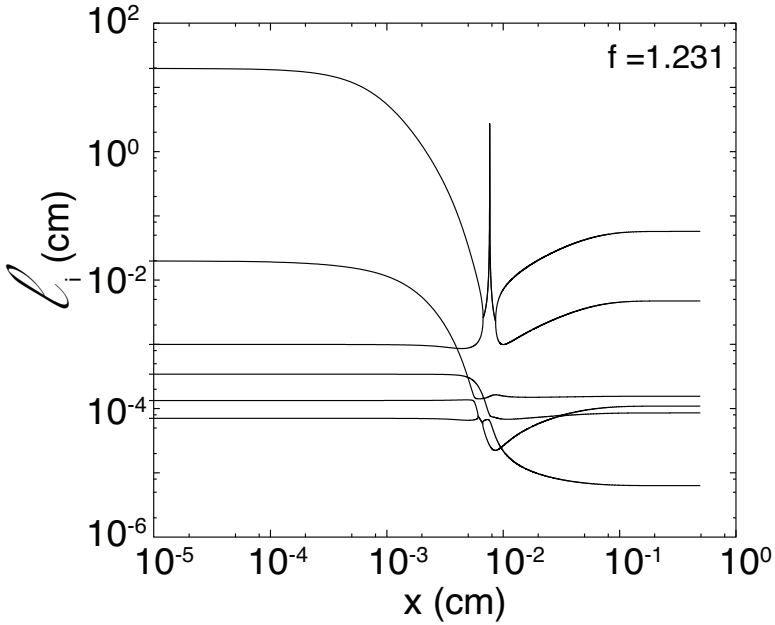

Using $L_{min} = 6.3 \times 10^{-6}\ cm$ from the higher overdrive and $L_{max} = 8.3 \times 10^{1}\ cm$ from the lower overdrive, the largest ratio of $L_{max}/L_{min} = 1.3 \times 10^{7}$. The ratio of the maximum to minimum induction zone length is 1.74.

$f = 1.08$

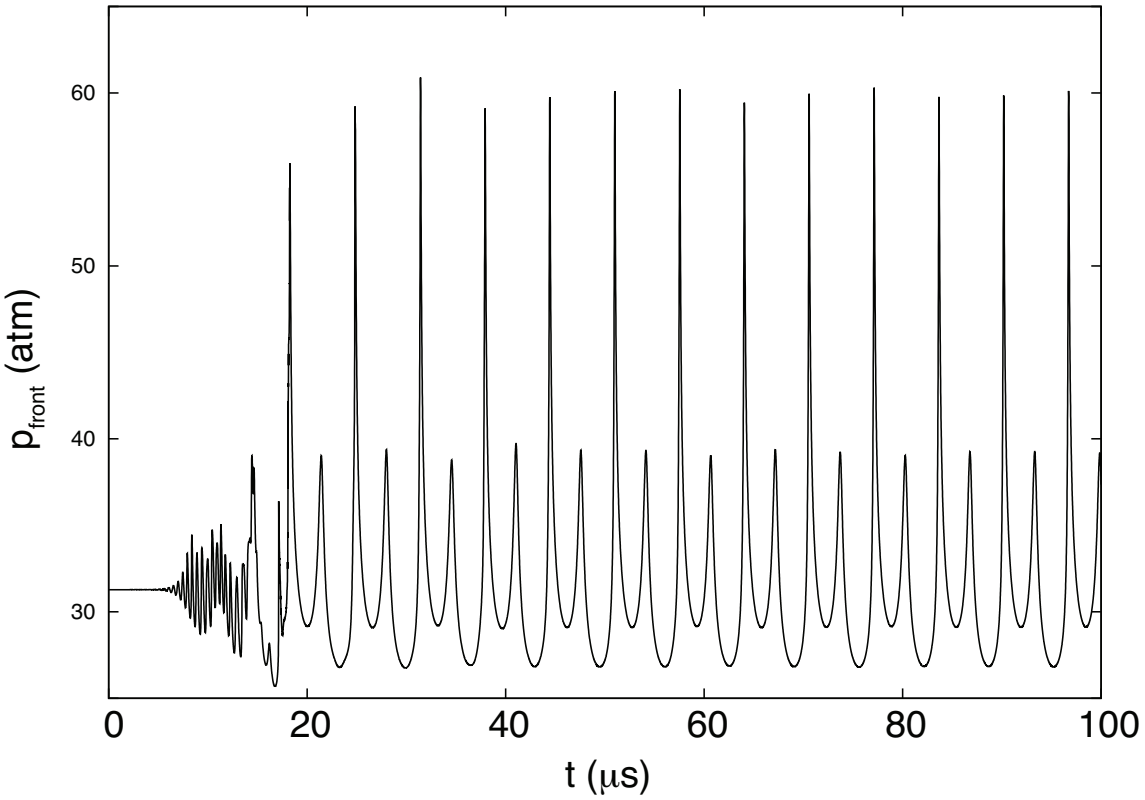

The detonation pressure has gone through a bifurcation, yielding a nearly period-2 detonation. Additionally, the amplitude of oscillations has increased.

$f = 1.08$ - Length Scales

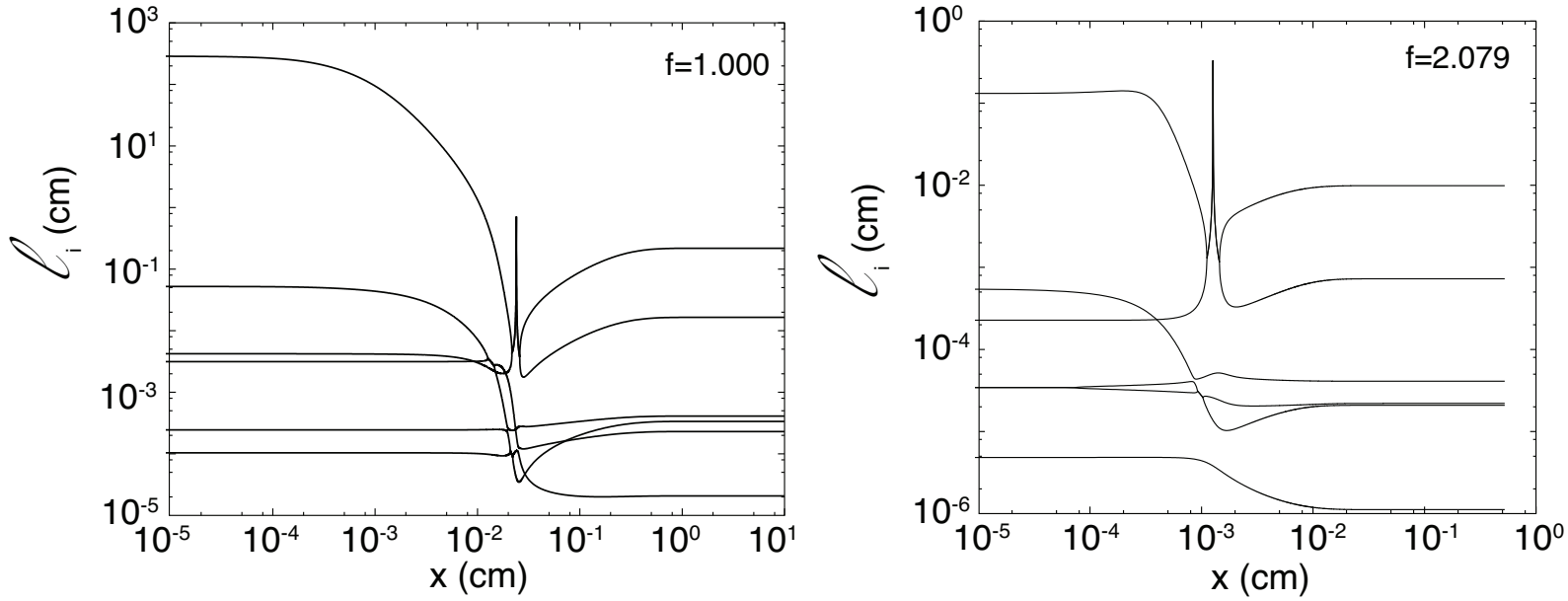

Since the lower overdrive is below the CJ detonation velocity, we are unable to obtain a length scale approximation at this overdrive; thus, we will use the length scales given by the near CJ detonation. With $L_{min} = 1.1 \times 10^{-6}\ cm$ occuring at the higher overdrive and $L_{max} = 2.9 \times 10^{2}\ cm$ occuring at the near CJ conditions, yields the largest ratio of $L_{max}/L_{min} = 2.6 \times 10^{8}$. The ratio of the maximum to minimum induction zone length is 13.1.

Conclusions

- Even small changes in activation energy can yield dramatic changes in the inherent length and time scales in detonation initiation in the one-step model
- The addition of diffusion reduces the time and distance to detonation; however, as more realistic viscosities are used, the inherent scales begin to approach those in the inviscid limit for detonation initiation
- In an already-initiated detonation, the predicted $L_{1/2}$ can vary significantly in a time-dependent calculation with ratio of the maximum to minimum $L_{1/2}$ growing as activation energy increases; the addition of diffusion reduces this ratio at a given activation energy
- Diffusive effects play a larger role in the initiation than in the propagation of a one-step detonation
- As the overdrive in a hydrogen-air detonation is lowered, the ratio of the length scales increases, similar to that predicted in the one-step model as activation energy increases